UNIVERSITÀ DEGLI STUDI DI PADOVA
DIPARTIMENTO DI INGEGNERIA CIVILE, EDILE E AMBIENTALE
Department of Civil, Environmental and Architectural Engineering

Corso di Laurea Magistrale in Environmental Engineering

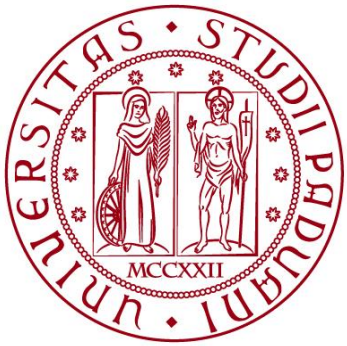

Investigation of Metal Particles in Aerosols

AHMED SALEH YASLAM BALFAQIH [1]

Master Thesis

Consortium for Aerosol Science and Technology (CAST) & Department of Physics, Division of Nuclear Physics. Lund University

Supervisor: Adam Kristensson[2]
Supervisor: Alberto Pivato[3]

Assistant Supervisors:
Axel Eriksson, Department of Ergonomics and Aerosol Technology.
Erik Ahlberg, Department of Nuclear Physics.

Academic Year 2022/2023

[1] ahmedsalehyaslam.balfaqih@studenti.unipd.it
[2] adam.kristensson@nuclear.lu.se
[3] alberto.pivato@unipd.it

DEDICATION

Specially dedicated to my beloved parents,

To my beloved siblings,

Dr. Yaslam, Eng. Abdullah and Eng. Mohammed Eng.Abobakr

To my beloved supervisors,

Prof. Dr, Adam Kristensson

Prof.Dr, Alberto Pivato

To all my friends and colleagues,

For all their encouragement, patience, and unconditional support, the hope that it will make a meaningful contribution to the field and pave the way for future research.

ACKNOWLEDGEMENT

First and foremost, Alhamdulillah, for granting me the strength and perseverance to complete my thesis. I am humbled and honored to express my most sincere gratitude to the individuals who have made this journey of writing my thesis an unforgettable one.

I am greatly indebted to my thesis supervisors, Prof. Dr. Adam Kristensson, and Prof . Dr. Alberto Pivato for their exceptional guidance, wisdom, and unwavering support throughout the entire process. Their expertise and knowledge in the field, coupled with their patience and understanding, were invaluable in shaping this work and helping me to reach my full potential. I cannot thank him enough for their mentorship and encouragement. I also sincerely thank Dr. Adam for taking the time to proofread and correct my mistakes. I am honored and fortunate to have had the opportunity to work with him.

I would also like to extend my sincerest appreciation to Axel Eriksson, Erik Ahlberg, and Patrik Nilsson for their valuable support and feedback, during my internship. Their contributions have been essential in not only improving the quality of this work but also my personal growth as a researcher. I am also grateful to Michal and Tobias (ICOS team) for the time I spend there during the campaign and also for the Fika we had.

My family and friends have been my source of strength and motivation throughout the entire journey. Their love, support, and understanding have been a constant reminder of why I embarked on this journey in the first place. They have been my rock, and I am eternally grateful for their unwavering belief in me.

Finally, I would like to express my deepest appreciation to all those who have been a part of this journey, whether directly or indirectly. This thesis is a culmination of their contributions, and I am forever grateful for their support and encouragement.

Thank you all from the bottom of my heart.

TABLE OF CONTENT

ABSTRACT

Air pollution is a major environmental concern that has a wide range of negative impacts on human health and the natural environment. One aspect of air pollution that has received significant attention in recent years is the presence of metal pollutants, such as lead and cadmium. Landskrona for a long time had problems with high concentrations of such heavy metals in the air. To investigate the air quality in terms of heavy metals in Landskrona, high time resolution multi-metals monitor (Xact 625i) was used to measure ambient air in two different locations (Urban background station at Lund city and rural background station at Hyltemossa) between 15 September and 3 October and between 19 October and 19 November 2022 respectively. Using online X-ray fluorescence spectroscopy of 240 minutes time resolutions. The results from the XAC show, elevated concentrations of Cu, Ni, Cr, and Pb were measured several times in both the city of Lund and Hyltemossa. Compared to previous campaigns for urban emissions, there is a clear downward trend in average element concentrations. In contrast, compared to the 2008 average concentrations for Cl and Cu from 2017, 2008, and 1988, there is an increase, but this is likely due to more winds from ocean areas in this study giving relatively higher contribution from the sea spray source. For the rural background measurements in Hyltemossa, V, Cr, Ni, Cu, Sr, and Pb were higher on average than for the Vavihill rural measurements during 2000. This was likely due to more frequent winds from continental polluted regions in this study. A few individual samples with high levels of heavy metal concentrations can significantly affect the overall average concentrations. Although these elevated concentrations do not exceed the annual limit set by environmental quality standards, it does not necessarily mean they are safe. The trajectories suggest that these heavy metal concentrations mostly come from long-range sources in Central Europe, but there could also be local or near-regional sources, such as wood combustion. However, this study was unable to confirm this, besides the wood combustion source which is considered as local or near-regional.

1.0 INTRODUCTION AND BACKGROUND

1.1 Health and Climate Effects of Aerosol Particles

Ambient particulate matter (PM) is a complex mixture consisting of several chemical constituents such as carbonaceous, ionic, and elemental species derived from both natural and anthropogenic sources, e.g., industrial facilities, incineration, vehicle exhaust, power plants, domestic heating, etc. Fine particles with a smaller diameter of 2.5 μm (PM2.5) have a direct relationship with human health because they can enter the bloodstream through the human respiratory system. These particles cause a wide range of harmful health effects, diseases, and disorders, including respiratory and pulmonary disorders, Alzheimer's disease, neurological toxicity, cancer, and even death (Kelly, F. J.et al, 2020). According to Squizzato, S.et al, (2018), long-term exposure to PM2.5 increases lung cancer deaths and deaths of cardiovascular diseases by 8, and 6 %, respectively for every 10 $\mu g/m^3$ increase of PM2.5 concentration.

Despite the necessity of clean air for human health and well-being, about 99% of the world population in 2019 was living in places where the WHO air quality guidelines (AQG) levels were not met (Ambient (outdoor) air pollution 2022). Air pollution is among the top five risks to human health (Juginović, A., et al, 2021). According to the Global Burden of Disease (GBD) assessment (2019), and according to World Health Organization (WHO) 2021, air pollution contributes to about 7 million deaths annually, where both indoor and outdoor pollution are attributed to that estimation. Even in Nordic countries, despite relatively low levels of air pollution, air pollutants have been estimated to cause around 10,000 excess deaths every year (Rittner, R., et al, 2020).

In addition to their health effects, aerosol particles also affect climate through interactions with clouds and solar radiation. The increase in anthropogenic aerosol particle interaction is supposed to lead to a negative radiative climate forcing through light scattering and through the formation of cloud droplets and clouds, which effectively scatter solar radiation. The estimated negative forcing may compensate for about half of the positive forcing of carbon dioxide (Su, H., et al. 2020).

From a global perspective, fossil fuel emissions have a large role in contributing to climate cooling by anthropogenic aerosols. Since aerosols affect the hydrological cycle, the removal of anthropogenic emissions leads to an increase in rainfall levels. (Lelieveld, J., et al. 2019). In other words, the reduction of fossil fuels-related aerosol emissions and other anthropogenic emissions affects positively saves lives and restores aerosol-perturbed rainfall patterns. However, the “global dimming” of aerosols will be diminished at the same time, leading to accelerated warming. Specific aerosol particles, for example, soot particles from combustion have a warming effect due to light absorption, and reducing these together with the greenhouse gases would be a win-win effect for climate change (Liu, et al.2020, Fuller, et al. 2022 and Lelieveld, et al. 2019).

1.2 Urban and Background Environments

As it’s known that the concentration of pollutants is varying from one air pollutant station and is based on the surrounding environment and pollution sources. For example, local emissions from road traffic make an appreciable contribution to overall air pollution in the urban area, but other anthropogenic emissions are also important. The contribution of road traffic emissions

happens via primary emissions of gases or particles, but also through the secondary formation. These take place after chemical gaseous reactions or when gaseous emissions transform into solid or liquid aerosol particles a long time after the first emissions (Harrison, R. et al, 2021).

Pollutants are also able to travel long distances in the air. (Weinzierl, B., et al, 2017). To be able to account for exposure to long-range transport (LRT) pollution sources at background locations and separate these sources from local pollution sources in the urban area, it is of vital importance to measure pollution levels where there is a gradient in pollution levels. For example, to estimate the contribution from the roadside pollution increment, air pollutant levels at this highly polluted site can be subtracted from levels measured at an urban background site. Similarly, the urban background increment can be estimated through subtraction of these levels and those measured at a regional background location. This provides an estimate of the influence of these sources on urban air quality. Figure 1 conceptually shows the variation of pollutant levels in different parts of the urban area. In general, the urban background represents the levels that most of the city dwellers are exposed to.

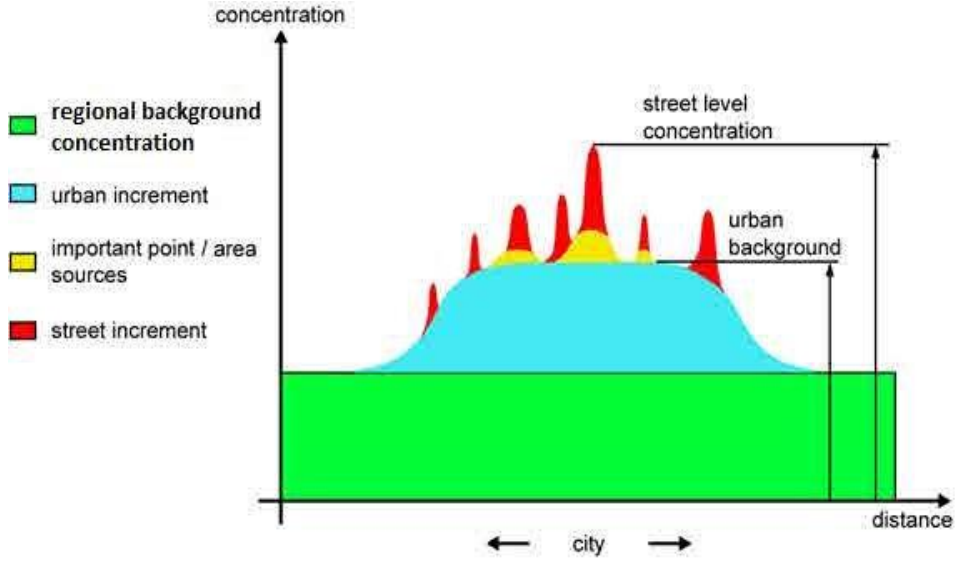

Figure 1 A graphic representation of the Spatial variation of air pollutants Pilla, F., & Broderick, B. (2015).

1.3 Aerosol Particle Air Quality in Southern Sweden

The air pollutant that causes the majority of premature death cases is anthropogenic aerosol particles. These are a mixture of local anthrophonic sources contributing to urban air quality as mentioned before, as well as LRT sources of both anthropogenic and natural origin, such as sea salt, mineral dust, agricultural emissions, and biological particles.

The Anthropogenic aerosols originating from the fossil fuels burning process receive high attention as climate-forcing factors and lead to cause adverse health effects. However, the variability and trends of aerosols originating from natural sources should be quantified to properly separate the impact of anthropogenic aerosol particles on the climate system and human health (Tegen, I., & Schepanski, K 2018).

Significant sources of aerosol particles in northern Europe are fossil fuel combustion from ships, road vehicles, coal power plant emissions, domestic and power plant biomass combustion, and forest fires. Natural sources are sea spray aerosols, and primary biological particles, such as pollen, virus, bacteria, and fungal spores. Secondary particles can come from agricultural emissions of ammonia, and forest emissions of biogenic volatile organic gaseous compounds (BVOCs). Dust can be regarded as both a natural and an anthropogenic aerosol particle source. These particles might come from resuspension from the Saharan desert, agricultural dust over bare agricultural areas in spring and during harvest time and road dust.

In southern Sweden, there is a significant contribution both from locally emitted particles, as well as particles through LRT due to the proximity to the European continent. The average mass concentration of particles smaller than 2.5 μm in diameter (PM2.5) in the road increment and urban background Malmö, measured at a heavily trafficked street Dalaplan, and on the rooftop of the city hall during 2019 was 10 and 9 $\mu g/m^3$ respectively (Spanne and Gustafsson, 2020). The corresponding value for rural background concentrations measured at Hallahus, about 45 km to the north of Malmö town, was 7.5 $\mu g/m^3$ (data from Swedish-EPA, 2020). This means that LRT contributed 7.5 $\mu g/m^3$ to the population exposure in Malmö town and the countryside in Scania. The local urban pollution contributed to 1.5 $\mu g/m^3$ (9-7.5 $\mu g/m^3$) in Malmö town, while the road increment at Dalaplan, was 1 $\mu g/m^3$ (10-9 $\mu g/m^3$). In other words, LRT is the strongest source of particles in Malmö town, at least for the yearly averaged PM2.5 mass concentration.

As presented by Johansson, F. (2018), long-range transported air masses passing Copenhagen contributed to increasing the concentration at Vavihill rural field station in the northwestern part of Scania. Particle number and black carbon (BC) mass concentrations were increased by 36% and 33 % respectively when air passed over Copenhagen compared to when the air missed Copenhagen. Particle number is dominated by small nanoparticles, and a higher number of these particles have special detrimental effects on human health due to their possibility to enter the bloodstream (Twigg, B. et al. 2009). BC particles are one of the most health-hazardous particles found in toxicological studies (Grahame, et al 2014 and Hakkarainen, et al 2022). However, the strongest anthropogenic contribution to high PM2.5 and BC mass concentrations occurs when the air comes from Eastern Europe. Not only are the emissions of these particles high from this source region (Yam, K. M. 2019), but the meteorological situation favorable for transporting the pollutants from eastern Europe to Sweden, is often associated with high-pressure systems not able to clean the air pollutants through mixing with air from above and with rain events.

According to Yam, K. M. (2019), the concentration of BC was on average about 370 ng/m3 and 190 ng/m3 for Dalaplan station and Hyltemossa station, about 50 km to the north-east of Malmö. At Dalaplan, the concentration rose to above 500 ng/m^3 during peak traffic rush hours (Figure 2). The Hyltemossa concentration increased from about 170 ng/m3 to 220 ng/m3 between day and night, indicative of the importance of domestic wood combustion as one of the most prominent sources.

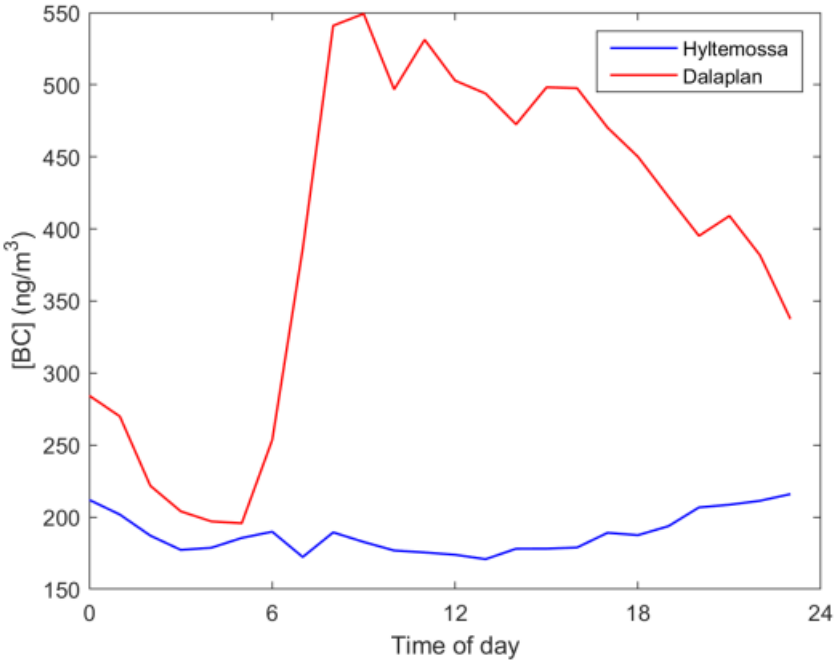

Figure 2 Diurnal variations of the median of [BC] at Hyltemossa and Dalaplan station in 2018

1.4 Health Effects of metal particles and Concentrations in Southern Sweden

Certain elements present in various aerosol particles have specific health effects and effects on ecosystems. Take Cu and Zn, for example, which are considered toxic elements, especially at elevated concentrations (Flemming and Trevors, 1989). The same is true for lead, which, once the pollutants enter the biologically during the deposition process, can lead to toxic effects and severe poisoning, since it is not an essential element for plants and has no biological function (Demayo et al., 1982).

Inhalation of copper nanoparticles can damage the kidneys, liver, and spleen (Chen, Z. et al. 2006). Long-term inhalation of copper can also cause nose, skin, and eye irritation, as well as headache, dizziness, and nausea (ATSDR 2022). Zinc exposure causes metal fume fever, decreased pulmonary function, chest pain, and cough (Truncale, T., et al 2015).

Lead can be absorbed through the respiratory tract and spread to soft tissue, the liver, and the central nervous system (Kumar Das, et al. 2011). Both the International Agency for Research on Cancer (IARC) and the Environmental Protection Agency (EPA) classify lead as a carcinogen (Harbison et al. 2015 & Kumar Das et al. 2011).

Respiratory irritation is associated with inhalation of tin, selenium, aluminum, iron, germanium, antimony, nickel, and strontium and prolonged exposure to tin can cause stenosis. alkali and alkaline earth metals such as calcium can cause mild to moderate skin and eye irritation, and chronic inhalation can cause liquefaction necrosis of soft tissues (Truncale, T., et al 2015).

WHO (2021) has recommended limit values for the protection of health due to PM and a few metals, whereas the EU (EEA, 2021) has put air quality limit values which are legislative and must not be exceeded (Table 1). Those recommendations for specific air pollutant limit values are based on evidence that leads to population health protection from the harm caused by air pollution. Also, the WHO guidelines on PM levels for the protection of human health have been recently updated (WHO,2021).

Table 1 Environmental quality guideline, limit values are based on annually exposure

Toxic metal	WHO	EEA	Reverence
	ng /m^3	ng /m^3	
PM 2.5	5000		WHO 2021
PM 10	15000		WHO 2021
PM 2.5		25000	EEA ,2022
PM 10		40000	EEA ,2021
Arsenic (As)	6.6	6	EEA ,2021
Cadmium (Cd)	5	5	EEA ,2021
Lead (Pb)	500	500	EEA ,2021
Nickel (Ni)	25	20	EEA ,2021

1.5 Previous Measurements in Landskrona

Aerosol measurements in the Landskrona region in southern Sweden have been made over several measurement periods since 1977 using two techniques: Falling dust sampling and aerosol sampling (Prosper, 2017). The falling dust sampling method has been the main measurement method since 1988, while aerosol sampling has usually been conducted at separate intervals of several years based on campaigns. The data obtained in 1977 showed a higher concentration of some heavy elements such as zinc, lead, and copper, while the concentration of the same elements decreased drastically in 1988. The reason for the decrease in lead concentration in 1988 is that Sweden initiated phasing out of leaded gasoline in the 1970s to protect the environment and public health. (Grönqvist, et al.2017). This contributed to about 80% decrease in lead concentration from 120 ng/m^3 to 25 ng/m^3 between 1977 and 1988 (Prosper, 2017).

Table 2 shows the concentration of three different elements measured in 2017 at two different sites, an urban background environmental site “Stadshuset” and an industrial site “Lundåkrahamnen”, for both fine (PM2.2) and coarse (PM10- PM2.2) particulate matter. Pb has been selected in the table due to its toxicity, Fe due to its relation to dust, and K due to its relation to domestic wood combustion. PIXE (Particle Induced X-ray Emission) technology was used at that time. (Kristensson, et al., 2019)

Table 2 Average concentration of lead, iron, and pota
ssium measured in Stadshuset and Lundåkrahamnen in Landskrona in ng /m3 during 2017 (Kristensson, et al., 2019).

Element	Fine fraction Stadshuset	Coarse fraction Stadshuset	Fine fraction Lundåkrahamnen	Coarse fraction Lundåkrahamnen
Pb	3.9	4.4	14	21
Fe	51	127	60	127
K	67	58	68	68

1.6 PARTICLES ELEMENT ANALYSIS WITH X-RAY FLUORESCENCE AND PARTICLE-INDUCED X-RAY EMISSION

Physical analysis techniques have shown great potential in elemental particle analysis often introducing a high sensitivity. Examples are atomic absorption and emission, X-ray fluorescence, and mass spectrometry. The Division of Nuclear Physics at Lund University has also invented PIXE, which stands for Particle Induced X-ray Emission. See section 2.7 for more details.

Historically PIXE has delivered high sensitivity and absolute quantification. Even though the sample spot is small. PIXE is capable not only to give average concentration but also it helps to study the variation over the surface of samples. one drawback of the PIXE method is that it requires a dedicated accelerator laboratory with a lengthy manual analysis of each particle filter sample.

The new online XRF technique with the Xact 625i instrument, which means the possibility to acquire direct results while sampling particles on a filter strap have emerged as a viable alternative to PIXE or offline XRF techniques. The Xact 625 uses energy-dispersive X-ray fluorescence analysis (EDXRF) and a low-power X-ray source. EDXRF allows rapid acquisition of the entire X-ray spectrum so that many elements can be detected within a few seconds. It has been proven that XRF technology is accurate, fast, and non-destructive, capable of achieving high time resolution while it does not require treatment of samples (Wang, F., et al,2021), which are some reasons why the Xact instrument is used by more and more laboratories rather quickly. However, there are only a few studies of the instrument's performance so far.

According to Liu, Y., et al (2019), Xact remained reliable and steady during their studied campaign in 2016. Also, it showed a similar result during the comparison with inductively coupled plasma mass spectrometry (ICP-MS) in all cases in 2016 with an average R^2 of 0.93 and an average slope of 1.07 for the elements As, Ba, Ca, Cr, Cu, Fe, K, Mn, Ni, Pb, Se, Sr, Ti, V and Zn. (Tremper, A et al, 2018).

XACT has a lower limit of detection (LOD) than equivalent laboratory-based methods, it also has shown a strong correlation to off-line filter-based Energy Dispersive X-ray Fluorescence (ED-XRF, which is one of two general types of X-ray fluorescence techniques used for applications in elemental analysis), ICP-MS as well as ICP-OES (inductively coupled plasma optical emission spectrometry). (Furger et al., 2017; Park et al., 2014; US-EPA, 2012).

1.7 OBJECTIVES OF THE STUDY

- Study the elements in the urban background air in Lund City using XRF data and look at the backward trajectories of the air masses to see where the air is coming from.
- Study the elements in rural background air in Hyltemossa from XRF data and look at the backward trajectories of the air masses to see where the air is coming from.
- To investigate the effects of exposure to metal-containing aerosol on the environment and health system. The intention is also to provide source marker data for subsequent source/receptor modeling that quantifies source apportionment.
- To collect PIXE filter samples to be able to compare with the Xact measurements at a later stage.

2.0 THEORY

2.1 AEROSOLS AND PARTICLES

An aerosol is a suspension of solid or liquid particles in a gas, and the gas itself, usually air. The particles, called aerosol particles, are usually prevailing for at least a few seconds in the air and some cases a year or more. The air around us typically contains a large number of particles from a variety of sources including smog in urban areas, photochemically formed particles, sea spray particles, and emissions from roadways including car exhaust particles from fossil fuel combustion. Aerosol particles play a fundamental role in affecting nature and health. Two of the most important are climate disruption and adverse health effects from inhalation in the human respiratory system.

The formation of aerosol particles in the atmosphere occurs in two main ways. First through direct particle emissions at the source or gas-to-particle conversion that takes place within a few seconds from the gaseous emissions. The particles are called primary particles. The particles can also be formed minutes up to days after the gaseous emissions through gas-to-particle conversion, and then these particles are referred to as secondary particles, Primary particles can be either biologically generated, such as bacteria, pollen, and fungi (Fennelly, et al., 2017), particles released during combustion, as in the car exhaust example above, or mechanically generated, such as windblown soil dust, abrasion of road surfaces by car tires, and by wave action over the sea areas and oceans. Secondary particles are known to be generated by the condensation of gases on pre-existing particles and by the formation of new particles (or nucleation) from gaseous precursors (Kristensson, Adam 2005).

The diameters of aerosol particles in the atmosphere vary by orders of magnitude, ranging from 0.001 μm to 100 μm. Aerosol particles are usually classified by size, and four modes or size ranges (Table 3). The nucleation mode includes the smallest particles with diameters up to 10 nm, and consists mainly of particles formed by gas-to-particle conversion, either as primary particles formed directly at the source or sometime after emissions of gases. The Aitken mode, with particle diameters of 10-100 nm, is the second smallest mode, which is formed by condensational growth of nucleation mode particles or direct emission from for example mechanical generation or fossil fuel combustion. Sometimes, there are other definitions of particle separation between nucleation mode and Aitken mode, where the boundary is set to 20, 25 or 30 nm diameter. These two modes often have the highest concentrations in the atmosphere but do not account for a large fraction of the total mass of aerosol particles due to their small size. The accumulation mode, the second largest size mode, consists of particles with diameters from 100 to 1000 nm. They make up most of the aerosol surface in the atmosphere, as well as

most of the secondary aerosol particle material (see section 2.2). They are composed of directly emitted particles, or formed by condensational growth of Aitken mode particles, or formed through aerosol-cloud interactions with subsequent evaporation of cloud droplets. The largest form, the coarse fraction, is greater than 1 μm in diameter and usually accounts for most of the total mass of aerosol particles, where primary biological particles and mechanically generated particles are among the most important sources. A population of aerosols consisting of particles of only one size is called monodisperse, which basically can only happen in a manufacturing process. A population of aerosols covering a wider range of particle sizes is called polydisperse, and atmospheric particles are always polydisperse. (Seinfeld & Pandis 2016).

Table 3: Table listing the different aerosol particle size modes.

Mode	Diameter (nm)
Nucleation	0 - 10
Aitken	10-100
Accumulation	100 - 1000
Coarse	>1000

2. 2 PRIMARY PARTICLES SOURCES

The XRF and PIXE techniques can provide the elemental composition of aerosol particles from Al up to a few of the heaviest elements in the periodic system. Several aerosol sources provide high mass concentrations of these elements. Apart from health effects, these elements can also be used as source markers for various aerosol sources and hence can be used for the quantification of how much these sources contribute to the total mass concentration of aerosol particles in the population. Several of these sources will be described in the following sub-chapters.

2.2.1 Fossil Fuel Combustion

Fossil fuel combustion is the burning of fossil fuels, such as coal, oil, and natural gas, to produce energy. This energy is used for various purposes, including generating electricity, heating, transportation, and industry. However, fossil fuel combustion also releases greenhouse gases, such as carbon dioxide and methane, and particulate matter, including metal particles, which contribute to climate change and have negative impacts on human health. (Perera, F. 2018).

Different fossil fuels release different types of emissions, including carbon dioxide, sulfur dioxide, nitrogen oxides, and particulate matter, including metal particles. For example, coal combustion can release sodium (Na), calcium (Ca), magnesium (Mg), aluminum (Al), iron (Fe), chlorine (Cl), arsenic (As), selenium (Se), cadmium (Cd), chromium (Cr), copper (Cu), nickel (Ni), lead (Pb), mercury (Hg), and zinc (Zn). (Maciejczyk, et al.,2021). Oil combustion can also release metal particles, such as nickel (Ni) and vanadium (V). (Maciejczyk, et al.,2021 & Corbin, J. et al,2018). As well as iron (Fe), sodium (Na), and barium (Ba), which are specifically produced from heavy fuel oil (HFO) (Corbin, J. et al,2018).

2.2.2 Soil Dust

There are several modes of transport of particles by wind, depending primarily on particle size and wind speed (Figure 3). As wind speed increases, sand particles about 100 μm in diameter are the first to be moved by wind stress (Greeley, R., et al. 1984). After lifting, these particles hop along the surface in a process known as saltation (Shao, Y., et al. 2011), and the impact of these saltators on the soil surface can move particles of different sizes. Since the cohesive forces between the dust particles are very large compared to the aerodynamic forces, the dust particles are usually not directly lifted by the wind but are mainly ejected from the soil through the influence of the saltating particles (Shao, Y., et al. 2011). After ejection, the dust particles are susceptible to turbulent fluctuations and therefore typically enter short-term (~20 – 70 μm diameter) or long-term (< ~20 μm diameter) suspensions (Figure 3). Long-term suspended dust can remain in the atmosphere for weeks and thus be transported thousands of kilometers from the source (Miller.R et al., 2006).

Therefore, the transport of soil particles can be represented as a perpetual continuous phase in terms of particle size as well as wind speed, particle size, and size distribution of soil particles. A long-term suspension (< ~20 μm diameter), short-term suspension (~20 – 70 μm), jump (~70 – 500 μm), and creep (> ~500 μm) (Figure 3). Several source regions might have soil dust emissions, like deserts (Griffin,et al, 2007), or sandy, and dry agricultural soils where plants have not yet started to grow on them (Wei, B., & Yang, L. 2010). Desert dust outbreaks from Sahara reached Europe (Mallone, S.,et.al, 2011: Renzi, M., et.al, 2017) and have the potential to even reach Sweden (Ansmann et al,. 2003).

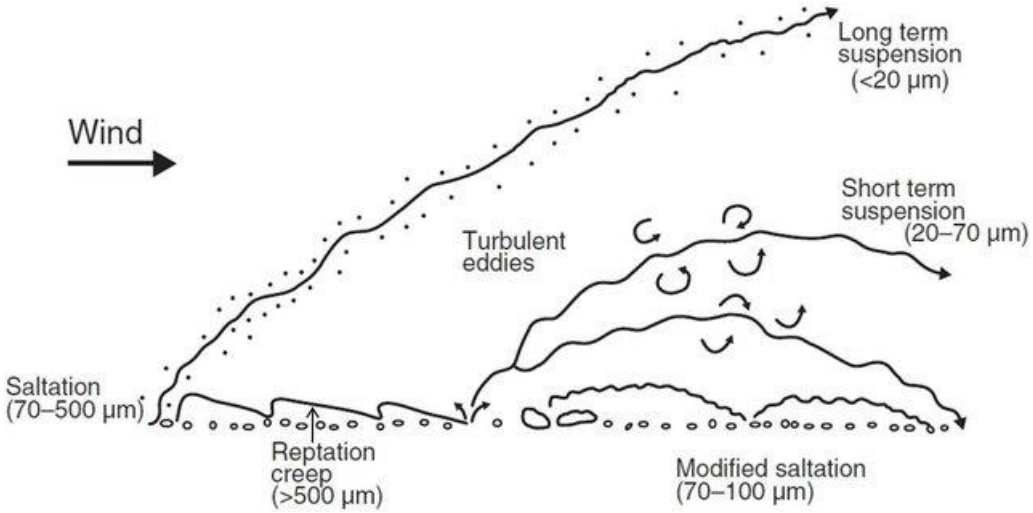

Figure 3 Schematic of the different modes of aeolian transport. Reprinted from Capulli, D., & Oliveira, E. N. D. M. N. (2014).

2.2.3 ROAD DUST

During the transportation of road vehicles, the contact of the wheels with the road surface leads to grinding processes on both the road surface and the wheels, resulting in emissions of particles into the atmosphere that can be inhaled. For example, road particles contain directly emitted sharp-edged metals such as lead, cadmium, zinc, barium, and nickel, as well as bitumen particles, which may be of particular interest for health effects (Bhardawaj, A.,et al,. 2017). Normally, this process occurs during dry periods in winter as studded tires and gritting materials

are used. When road surfaces dry out towards spring, a large amount of grit is thrown into the air and generates large mass concentrations of PM10 (Fullová, D., & Đurčanská, D. (2016).

2.2.4 SEA SPRAY

The ocean is a source of liquid particles, which are transformed by the friction of the wind on the surface of the sea into aerosols, which, once they reach the atmosphere, shrink by evaporation, and are enriched with sea salt and other substances contained in seawater. These particles are referred to as sea salt or more commonly sea spray since they may also contain organic material. Sea spray aerosols typically range in size from tens of nanometers (nm) to tens of micrometers (μm). There are two main mechanisms responsible for the emission of sea spray into the atmosphere: the bursting of air bubbles in the ocean (Figure 4a-b) and the wind breaking off wave crests (Figure 4c).

When the wind is strong enough, the friction of the wind on the ocean surface causes the water at the surface to move faster than the water below the surface, causing the wave to break. This traps air bubbles in the ocean, which can then rise to the surface and break up.

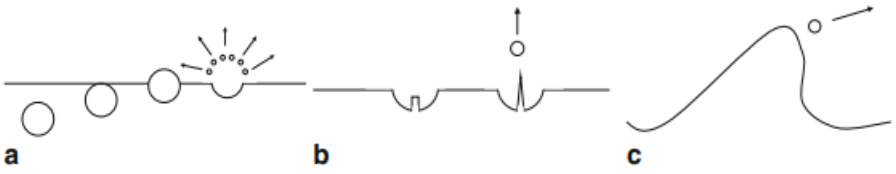

Figure 4 Schematic description of the three different source mechanisms for sea spray aerosols: (Adapted from Lewis and Schwartz (2004)) a) formation of film droplets, b) formation of jet droplets, and c) wind breaking of wave crests.

When many air bubbles are present, the ocean is covered with foam, also known as whitecaps (Lewis, et al.,2004 & Monahan, et al.,1983); however, air bubbles can also be present in much lower concentrations. Biological processes can also form air bubbles in the ocean, but this source is considered less important than the primary production factor, wind speed. The bursting of air bubbles at the ocean surface leads to the formation of seawater particles by two different mechanisms. When the water film around the bubble itself bursts, droplets are formed. Particles of relatively small size are thrown in all directions. These are called film droplets (Figure 4a).

When the interior of the burst bubble fills with water and a vertical jet form, some droplets are also ejected vertically. These are known as jet droplets (Figure 4b). Although this process only ejects a few droplets per air bubble, there are a large number of air bubbles whose size is optimal for causing jet droplet emission. Droplets can also be torn off the crests of breaking waves. These droplets are larger than those produced by the other two mechanisms and are referred to as spume droplets (Figure 4c) (O. Boucher, 2015).

2.2.5. Wood Combustion

Wood combustion is the process of burning wood to produce heat or electricity. Wood is often used as a renewable energy source to heat homes, businesses, and industrial facilities, and it can also be used to generate electricity in some power plants (Sahoo, K., et.al, 2021). It is a cheaper option for heating compared to other alternatives, especially in colder seasons. (Molnar,

et.al, 2005 & Trojanowski, R., & Fthenakis, V. 2019). However, residential wood combustion plants were responsible for over 45% of PM2.5 emissions in Europe in 2015 and similar trends were reported in Denmark, the number of particles per unit volume of exhaust from wood combustion plants was more than 230 times higher than that from diesel vehicles, (Heat, C. 2016). Which leads to a decline in local air quality (Hugony, F., et al. 2012).

According to Heat, C. (2016) domestic heating (primarily wood burning) accounts for more than half of Europe's black carbon emissions. According to projections, the relative share will rise to nearly 70% by 2030. Burning wood can release particulate matter in the form of small particles suspended in the air. These particles can have a variety of substances, including the volatile alkali metals K and Na (Van Lith, S. et al, 2006). Moreover, heavy metal particles are associated with domestic wood burning, including (Cd, Cr, Cu, Ni, Pb and Zn) (Olszowski, T., & Bożym, M. 2014). As well as S and Cl. (Van Lith, S. et al, 2006).
According to the study of Kocbach, A., et al. (2005), the results of X-ray microanalysis (XRMA) showed that potassium (K) and sulfur (S, from a reaction with gases in the ambient air) were the most abundant elements observed in the particles, while silicon (Si) and calcium (Ca) were present only in small amounts.

2.3 SECONDARY PARTICLES SOURCES

2.3.1 New Particle Formation

Nucleation or new particle formation (NPF) is one of the major sources of high concentrations of aerosol particles in the atmosphere. New particle formation refers to the production of new charged or neutral particles, 1 to 2 nm in diameter, as a result of a variety of conversions from gas to particles. It is estimated that about half of the global cloud condensation nuclei (CCN) are produced by nucleation after the growth by condensation of newly nucleated particles to sizes around 100 nm diameter (Merikanto et al. 2009). According to (Pettibone, A. J. 2009), NPFs are an important source of particles and could affect climate by changing their size distribution. There are several theories for the formation of new particles. The key process is called cluster activation and consists of three steps. The first step involves the formation of clusters through gas phase reactions. The second step is the homogeneous or ion-induced nucleation of neutral or ion clusters. The last step involves the growth of these clusters into larger particles. Figure 5 depicts the processes, as well as the diameters at which the various processes occur (Kulmala et al, 2013).

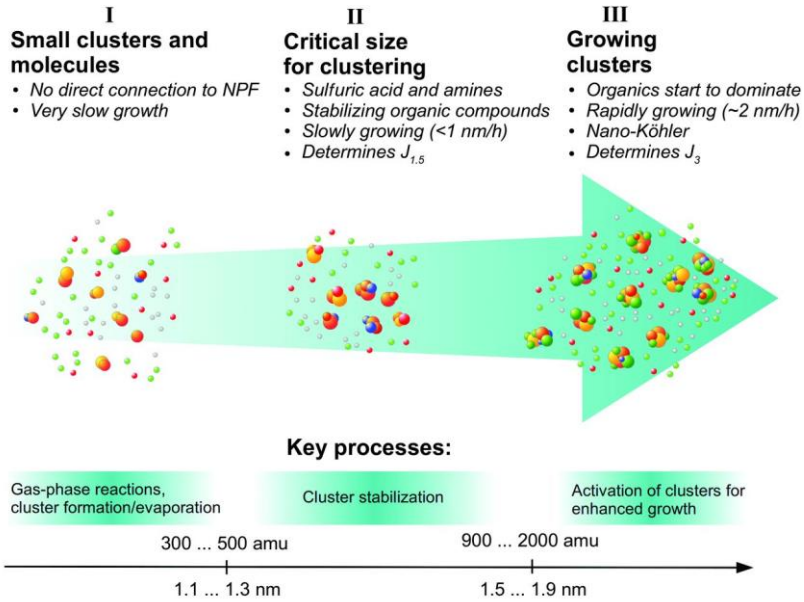

Figure 5 Schematic description of main size regimes of atmospheric neutral clusters and the main processes related to those size ranges. (Kulmala et al, 2013).

2.3.2 Condensation

Condensation is a process that occurs when a gas changes phase to a liquid. In the context of aerosols, condensation refers to the process by which water vapor in the air condenses onto small particles (Figure 6), forming droplets. This process is important in the formation and evolution of aerosols and can have a significant impact on air quality and climate. (Kolb & Worsnop, 2012).

Both organic and inorganic compounds can be present in the condensation process in the atmosphere and in aerosols. Organic compounds are those that contain carbon and are often found in living organisms or in materials derived from living organisms. such as emissions from vegetation, combustion of fossil fuels and or biomass (Glasius, M., & Goldstein, A. H. 2016). Inorganic compounds are those that do not contain carbon and are often found in non-living materials or in materials that are not derived from living organisms such as emission from volcanoes, natural fires, or industrial processes. When water vapor condenses onto small particles in the atmosphere, it can create droplets that contain both organic and inorganic compounds. The exact composition of the droplets will depend on the specific compounds that are present in the atmosphere at the time of condensation.

The presence of organic and inorganic compounds in condensation droplets can affect the properties and behavior of aerosols, including their size, composition, and optical properties. The interaction between organic and inorganic compounds in aerosols can also affect how aerosols interact with other atmospheric constituents, such as clouds and radiation. Kolb, C. E., & Worsnop, D. R. (2012).(Glasius, M., & Goldstein, A. H. 2016).

2.4 DYNAMICS OF AEROSOL PARTICLES

Primary and secondary aerosol particles undergo chemical and physical transformations during their early emission phase into the atmosphere, leading to different formation processes in terms of the composition and size of these particles.

2.4.1 Condensation / Evaporation

Condensation occurs when gases adhere to existing atmospheric particles in the atmosphere, increasing the mass concentration without changing the number concentration. The opposite process is called evaporation, in which aerosol particles shrink as gas evaporates from them. When a gas molecule condenses on the surface of an existing particle, it can either adhere to the surface or dissolve in the liquid interior of liquid aerosol particles. Because of the chemical reactions that take place in the liquid phase, this can result in altered chemical properties.

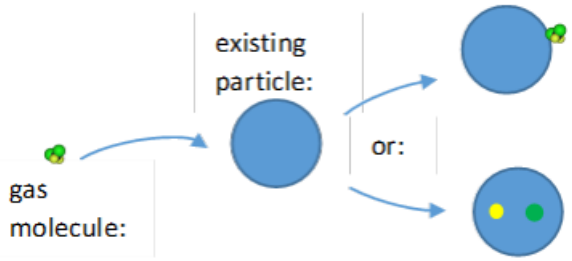

Figure 6 Principal drawing of condensation of gases onto pre-existing particles in the atmosphere

2.4.2 Coagulation

Coagulation occurs when two particles collide and adhere to each other due to collision. This reduces the number of aerosol particles in the atmosphere, but the mass concentration remains unchanged. At the same time, the new coagulated particle is larger than the original particle. As can be seen in Figure 7, the particles either dissolve into each other or form agglomerates. In addition, if one of the particles is solid, a solid core may form in the center of the new particle (Jacobson, M. Z., & Turco, R. P. 1995).

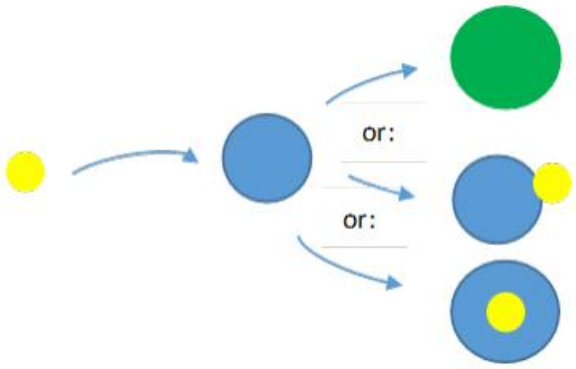

Figure 7 Principal drawing of the coagulation process between two particles

2.4.3 Dry and Wet Deposition

The deposition of air pollutants through its life cycle (Figure 8) is a significant factor that leads to the loss of both gas and aerosol particles in the atmosphere by capturing pollutants generated from both primary and secondary sources and depositing them onto the surface. (Lagzi, I., et al., 2013). There are two types of deposition processes, wet deposition, and dry deposition (Figure 9). Wet deposition is the most common method for removing aerosol particles, which is capable to removes 80-85% of them (Martin, A. et al,2021). Wet deposition predominates in areas with high annual precipitation, while dry deposition predominates in areas with low precipitation (Connan et al., 2012)

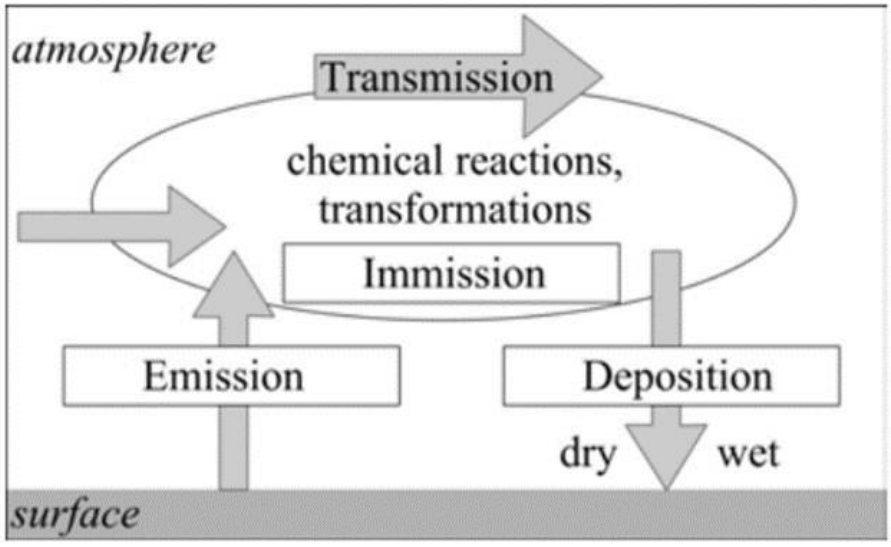

Figure 8 A schematic drawing showing life cycle of air pollutants (Lagzi, I., et al,2013)

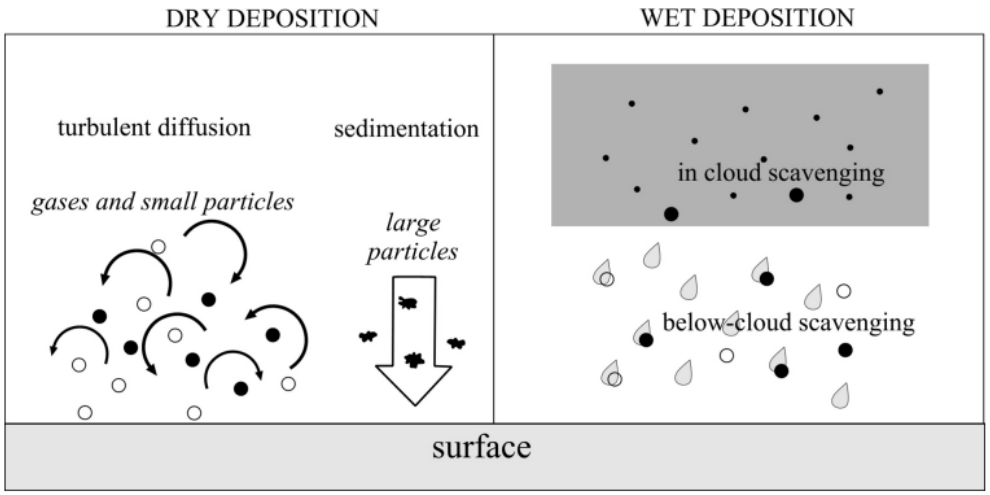

Figure 9 Dry and wet deposition processes in the atmosphere (Leelőssy, Á., et al, 2014)

2.4.4 WET DEPOSITION

The main sink of aerosols in the atmosphere, at least for soluble species, is wet deposition, also called wet scavenging. It includes both scavengings that occur within the clouds during the formation of precipitation (i.e., in-cloud scavenging), and scavenging that occurs under the cloud because of the downward flux of precipitating water (i.e., below-cloud scavenging). When a liquid water cloud forms in the atmosphere, a fraction of the aerosol is incorporated in the aqueous phase, either as a cloud condensation nuclei (water vapor condenses upon a hydrated aerosol particle and becomes a cloud droplet) or through impaction (an interstitial aerosol particle is incorporated into the aqueous phase during the collision with a cloud droplet). If cloud droplets grow to a size where their sedimentation velocity is large enough, the cloud starts to produce drizzle or precipitation, and aerosol matter that is incorporated in the falling droplets is scavenged. If the falling droplets (or drops) reach the surface, then the aerosol mass is removed from the atmosphere. (Boucher, O. 2015).

During their fall, raindrops sweep a volume of air and collide with a fraction of the aerosols that are present in this volume. This process, called below-cloud scavenging, occurs through Brownian diffusion, interception, and impaction (Duhanyan, N., & Roustan, Y. 2011), as shown in Figure 10. Brownian diffusion means that nanosized particles can deviate from the air currents around the droplets and affect the water surface. In addition, interception works when a larger aerosol particle passes along the air flow lines. If the particle is too close to the water surface, it will also impinge on the droplet. Impaction also works for larger particles and is the process by which the particles are forced to deviate from the airflow due to their inertia, thus impacting the droplet (Lagzi, I., et al., 2013).

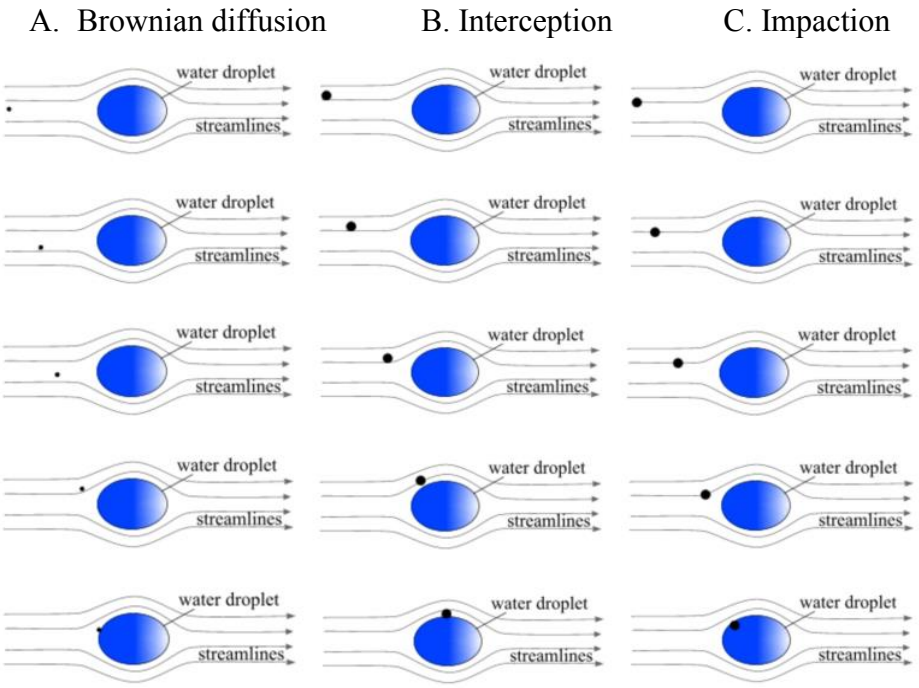

Figure 10 The sequence of impinging aerosol particles on water droplets, by a) Brownian diffusion, b) interception, and c) impaction. (Source: a document provided by Adam Kristensson,2022)

2.4.5 DRY DEPOSITION

Dry deposition represents the opposite process of wet deposition since it mainly occurs in the absence of precipitation events. According to Ruijgrok et al. (1995), dry deposition mainly occurs when the particles are relatively close to the ground or the surface objects, which can consist of multiple types of surfaces, for example, vegetation, water, and human constructions. Aerosol particles can also get deposited at the surface in the presence of fog or mist. In this case, aerosol particles are deposited together with the small water droplets that constitute the fog. (Boucher, O. 2015). Turbulent diffusion and Brownian diffusion are two mechanisms that can contribute to the deposition of particles to the ground, although each mechanism is more efficient at depositing certain size ranges of particles. For example, turbulent diffusion is more efficient at depositing larger particles, and Brownian diffusion is more efficient at depositing smaller particles. According to Mariraj Mohan, (2016), the prime mechanism for dry deposition is likely turbulent diffusion, Figure 8. The transport of mass, heat, or momentum within a system caused by random and chaotic time-dependent wind movements is referred to as turbulent diffusion (Seinfeld & Pandis 2016).

2.5 X-RAY FLUORESCENCE -XRF

The Xact 625I Ambient Metals Monitor (Cooper Environmental Services (CES)) is designed for high-time resolution multi-metals monitoring of ambient air, which measures up to 67 elements with atomic numbers between Aluminum (Al) and Uranium (U). The instrument works by sampling reel-to-reel filter tapes and then analyzing metals in the resulting particulate matter (PM) deposit with nondestructive X-ray fluorescence (XRF). The Xact 625i draws in ambient air via a PM size selective inlet and filter tape. While the next sample is being collected,

the resulting PM deposit is automatically advanced and analyzed by the XRF system for selected metals.

The Xact 625i takes continuous measurements for a user-specified sampling time (i.e., 15, 30, 60, 120, 180, or 240 minutes), which can be changed depending on the time resolution of the data required. Using energy-dispersive X-ray fluorescence (ED-XRF) spectroscopy, X-ray fluorescence (XRF) is a technique for identifying and quantifying the elements present in a sample.

X-ray fluorescence (XRF) is a way of finding out what elements are in a certain sample and how much of each element is present. It does this by irradiating high-energy photons, such as X-rays or γ-rays, at the sample (Santoso et al., 2010). When the atoms in the sample are hit by these X-rays, they give off their X-rays. These X-rays can be picked up and analyzed to tell us what elements are in the sample and how much of each element there is. This technique can be used to detect various elements in air pollution and help identify the source. (Santoso et al., 2014).

XRF spectroscopic analysis is a way to figure out what elements are in a material by looking at the unique X-rays that each element gives off. This is done by shining primary X-rays, which have specific energies, on the material. This causes the innermost electrons in the atoms of the material to get excited or ionized, and they give off secondary X-rays. These secondary X-rays are picked up by a detector and turned into electronic signals. A computer analyzes these signals and produces a spectrum that shows the elements present in the sample and their concentrations (Rixson et al., 2015). (See Figure 11). This data can be recorded in a report and can be downloaded from the XACT system.

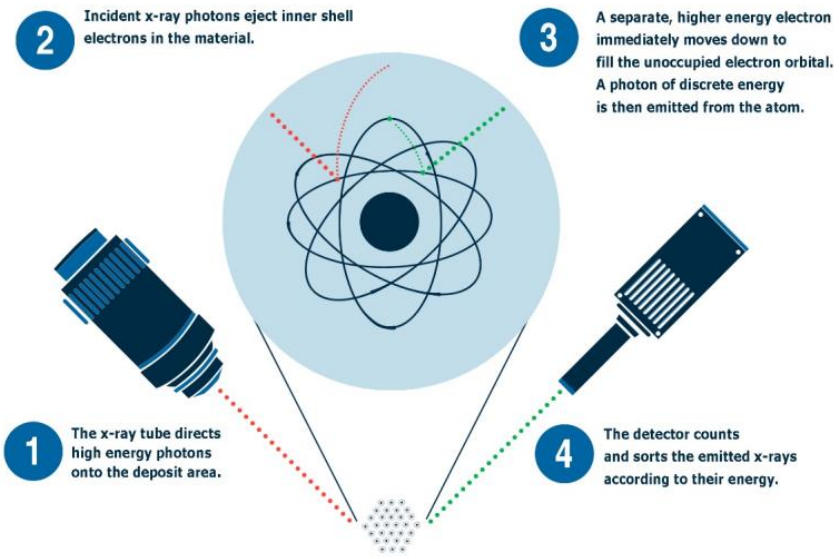

Figure 11 The XRF basic principle

As previously mentioned, Xact has been shown to produce similar average concentrations to other methods, e.g., inductively coupled plasma methods (Furger et al. 2017), the average daily concentration results of Xact will be compared to particle-induced X-ray emission (PIXE) results from 24-hour sampling.

2.6 PARTICLE INDUCED X-RAY EMISSION – PIXE

Particle-induced X-ray emission (PIXE) is a technique for analyzing elements using a characteristic X-ray emission. A proton beam is used to excite the electrons of the inner shell of an atom, creating vacancies in the inner shell. An excited atom strives for a stable energy state, and therefore, these vacancies are filled by electrons from the outer shell, producing X-rays (Figure 12). Since the X-rays correspond to the energy difference between the outer and inner shells, and these energies are characteristic of each element, the X-rays are detected and classified based on their energy using a semiconductor detector. The yield of characteristic X-rays is then converted to absolute concentrations of Al and heavier elements with detection limits of 0.05 ng m-3. (Kristensson, A. 2005). The proton beam used in PIXE's technique is nondestructive to samples and can be used on solids, liquids, and aerosol filters. (Prosper, W. 2017).

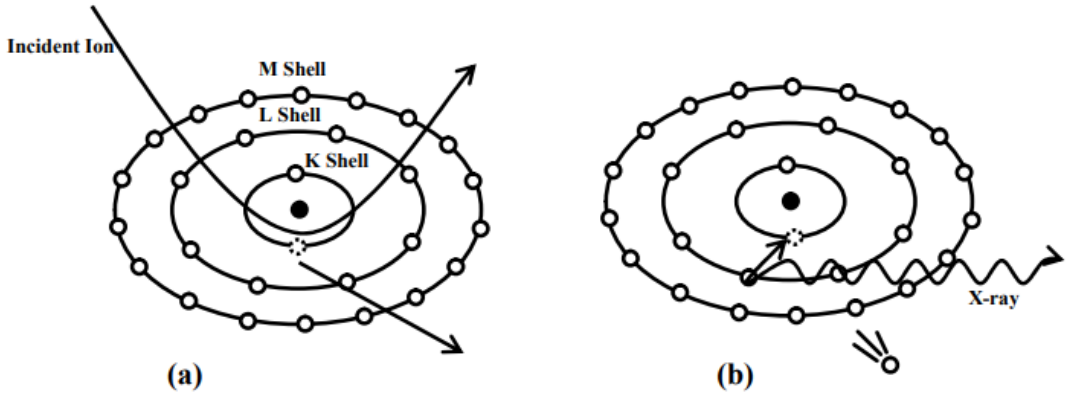

Figure 12 The PIXE basic principle. (a) Indicates ion interaction with an electron in the inner shell. (b) Indicates electron emission, upper shell electron fall, and x-ray radiation. Kabir, M. H. (2007).

3.0 METHODOLOGY

3.1 STUDY AREAS

3.1.1 SCANIA (SKÅNE)

Scania (Skåne) is Sweden's southernmost county, covering approximately 11,350 km^2, or about 2% of the country's total area (Figure. 13a). With approximately 1.4 million inhabitants (approximately 13% of the total Swedish population) (SCB 2021), it is one of the most densely populated regions in the country. Most people in Scania live in the west, where pollution levels are higher than in other parts of Sweden. This increased exposure is due to increased road transport to and from the European continent, as well as significant cargo shipping and ferry transport along the coast and the vicinity of the Copenhagen, Denmark area.

3.1.2 LUND CITY

Lund has a population of 92 000 residents (SCB 2021) and covers an area of 23 km^2, located in southern Sweden at 55°42'N, 13°12'E, 35 km NE from Malmö city. Malmö is Sweden's third largest city with 344 000 residents. Malmö is known as one of the cities with the highest levels of air pollution in Sweden. (Malmqvist et al. 2018, Gustafsson, M., et al. 2014). The university characterizes Lund City in many ways, and approximately one-third of the residents are students. As a result, the city's residents are younger than the national average, and the age group 20-29 is especially overrepresented. (Stroh, et al. 2005).

The study was carried out both at the urban background Lund and at the rural background station Hyltemossa, about 50 km north of Lund. In Lund, measurements were performed with both Xact and PIXE filter collection, and the measurement site was chosen in the parking lot behind the IKDC building (Figure 15a,15b), where there are usually few cars parked. Occasionally, however, there could be high levels of pollution if a car is idle in the vicinity of the particle inlet system. However, with four- and 24-hour filter collection with Xact and PIXE respectively collection, the impact of this contamination should be insignificant in most cases. In the Hyltemossa research station in northwestern Scania (Figure. 13b), Xact measurements were performed, but not PIXE filter collection. The station represents a rural background, located a few kilometers south of Perstorp Municipality (56°06N, 13°25E (115 m asl)). The forest in Hyltemossa is managed and dominated by Norway spruce (Picea abies) with a small percentage of Downy birch (Betula pubescens) and Scots pine (Pinus sylvestris). (ICOS 2022). The forest is between 13 and 19 m high and holds about 190 m3 per hectare (excluding branches, stumps, conifer biomass, and roots). It is about 4 years old. In 1981 the area was damaged by a storm, so it was cleared in 1982 and replanted in 1983 with 3300 trees per hectare. The XRF instrument was placed on the northern outskirts of this forest in a small marsh with humid conditions that is a pasture area for cows of about 60 m² (Figure 16a,16b). Around 300 m south of the station, there is about a 36 m² of clear-cut that was harvested in 2018. (Huskin Okinedo, P. 2020). To the north and east direction Lille Sjö Lake and Håkantorps and Mölledamm Lake are about 1400 m and 1500 m respectively away from the station. The Bjärröd countryside road is located about 500 m to the west direction with an estimation of 500 vehicles passing through that road per day. To the NW, about 3000 m away from the station there is a chemical manufacturing company (Celanese Emulsions Norden AB).

Figure 13 (a) Map of Scania area with inserted picture containing major towns and road network. Image by Emilie Stroh. (b) Map of Hyltemossa background station and Lund City Station

3.2. Instrument Setup and Aerosol Particles Sampling

As mentioned earlier, the aerosol particle samples were collected from two different locations. The first location was the aerosol laboratory parking lot at IKDC. Both Xact and PIXE were connected to a steel pipe, which is the main inlet for particles with a PM1 collection (see section 3.4). 33.4 l/m of air was drawn from the parking through a 10 mm tubing that has curves to prevent high-size particles from passing through during collection, with tube shape and dimensions Figure 14. The flow was split into two parts, one for PIXE filer collection, and the other for XACT. The PIXE filter collection flow was maintained with an external pump running on critical flow, while the Xact flow was controlled electronically without critical flow. Flow measurements were performed for Xact and PIXE filters during PIXE filter changes every 24 hours in the morning, both before and after the sampling time ended for both PIXE and XRF. The average of the start time and ending time flows is presented in (Table 4). As can be seen from the flows at the start and end, the PM1 mass concentration was not high enough to cause a significant drop in the PIXE filter flows during the measurement period.

Table 3 Average start and ending flow measurements of Xact and PIXE filter collection measured every 24 hours, before and after PIXE filter changes in the morning.

Instrument	Start flow l/min	Ending flow l/min
XACT	17.1	17.1
PIXE	16.4	16.4

The duration of XRF sampling was set to the maximum possible 240 minutes (4 hours) to compare the results with the 24-hour sampling results obtained from the particle-induced X-ray emission method (PIXE). Automatic calibration and quality assurance protocols took place for XACT at 0:00 for 30 minutes, which means that particle sampling was interrupted during this time. After calibration is complete, sampling resumed as usual at 0:30 AM. We tried to keep the PIXE filter change procedure time as short as possible. Old PIXE filters were put in Petri dishes covered with aluminum foil and stored in the freezer before sending them to the Lund Micro Pelletron facility to be analyzed. PIXE analysis has been performed, but the analysis was made too late to be able to include it in this report. Figure (15a) shows the Xact and the PIXE setup in the aerosol laboratory of IKDC. For the Hyltemossa measurements, the XRF was placed directly below a PM10 inlet at the roof of the measurement (Figure 16), with a flow rate of 17.1 l/min on average. Since the inlet is supposed to be driven by a 16.7 l/min flow rate to achieve a 10 µm diameter upper size cut-off, the true PM collection was for particles slightly smaller than 10 µm diameter.

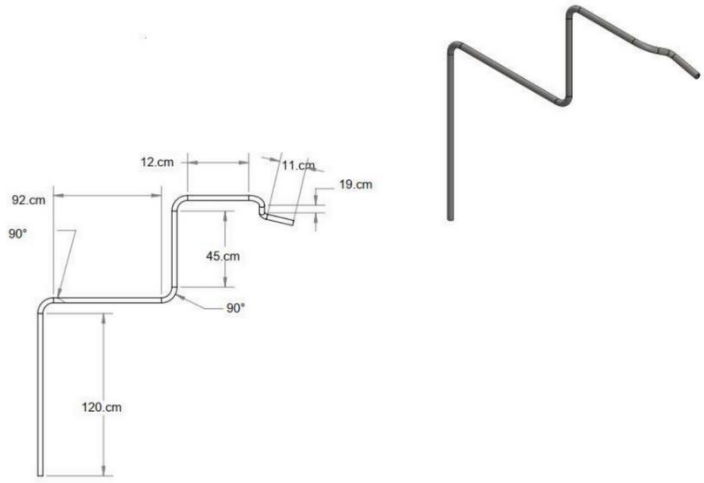

Figure 14 Inlet tube at IKDC building

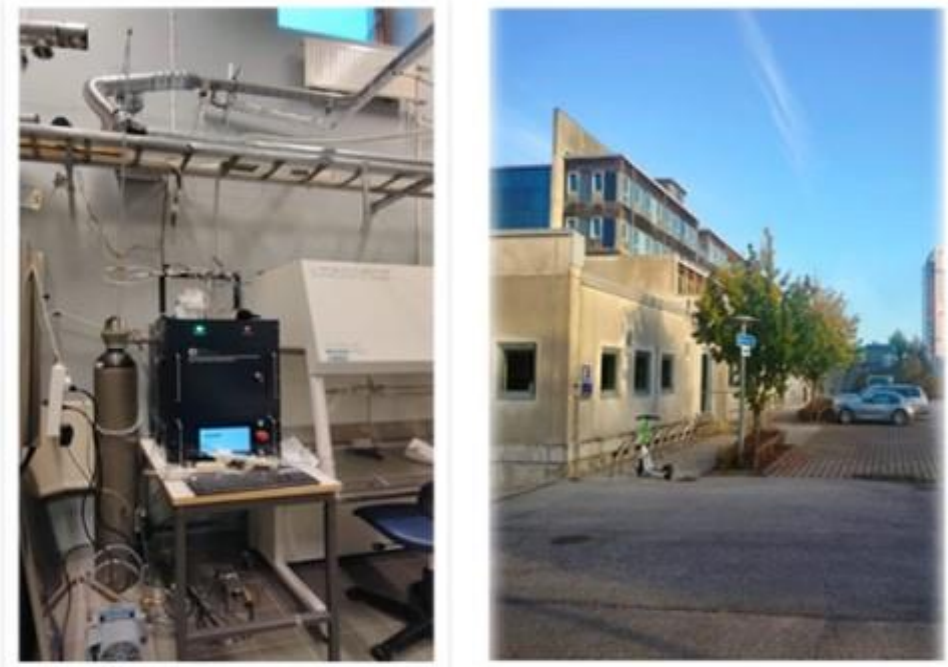

Figure 15 (a) Xact 625i Multi Metals Monitor and PIXE set up in the lab.
(b) Parking lot at IKDC

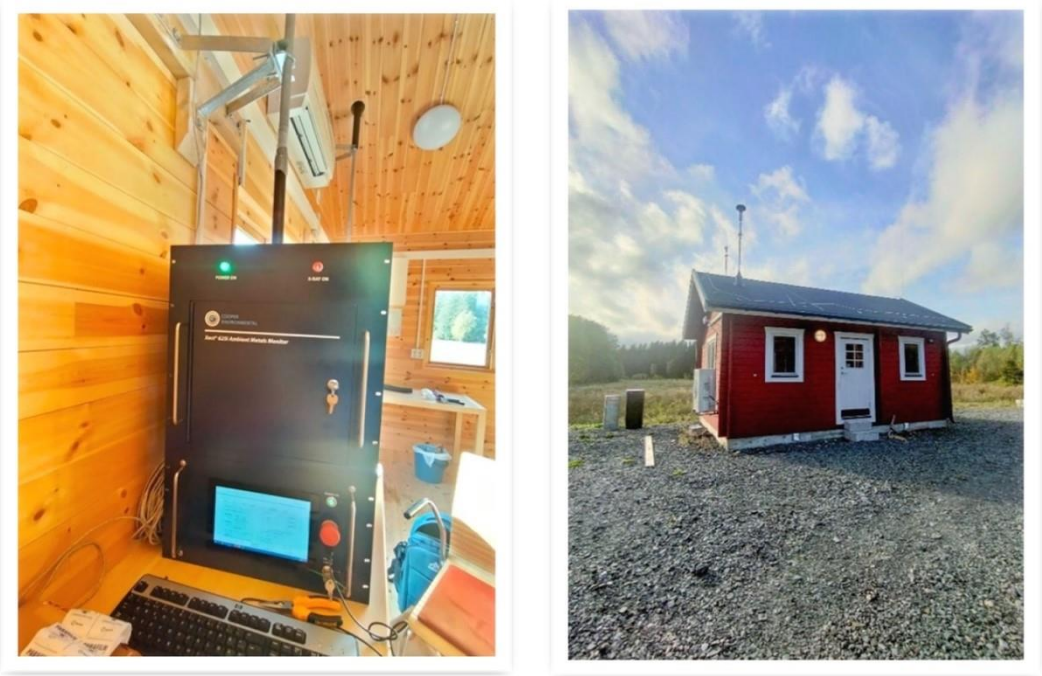

Figure 16 Xact 625i in the new hut at Hyltemossa station. (b) Hyltemossa monitoring background station. Photo By Ahmed Balfaqih

3.3. Measurements Period

An initial test run of the Xact for indoor air was conducted at the IKDC aerosol laboratory for three days to verify the sampling procedures of the Xact, with some cleaning in between. Two measurement campaigns were then conducted, one in the aerosol laboratory at IKDC to measure outdoor air collected in the parking lot for 19 days from September 15 to October 3, 2022, for both XRF and PIXE. In the second measurement period, Xact was transported to the Hyltemossa station, and a new filter was installed before starting the new sampling period, which began on October 19th for one month to 19 November 2022.

During this period, Xact sampling was interrupted due to a tape failure at 12:00 on October 29 and resumed at 14:00 on the same day. Same for the 8 and 9 of November from 8:00 and 11:09 and resumed at 10:55 and 12:13 respectively. Sampling was also interrupted after 20:00 on November 11 for unexplained reasons and reactivated the same day at 20:45.

3.4 PARTICLE LOSSES CALCULATION

The losses in the complicated inlet system in the Lund laboratory (Figure 14) were calculated theoretically with the loss calculator (Von der Weiden, et al, 2009). It included losses due to Brownian diffusion, sedimentation, impaction, and interception, and the flow in the tubing was calculated to be turbulent. All bends and lengths and widths of tubing were included in the loss calculation. This yielded an upper PM1 cut-off at the end of the particle collection system (Figure 17). There were also significant losses of smaller particles below 30 nm diameter, however since these do not contribute in a significant way to the aerosol mass, this effect was disregarded. Nevertheless, it should be noted that the particle collection efficiency was not 100

% for any size range as can be seen in Figure 17. The maximum efficiency was only about 93 % for the size range between roughly 30 and 300 nm diameter.

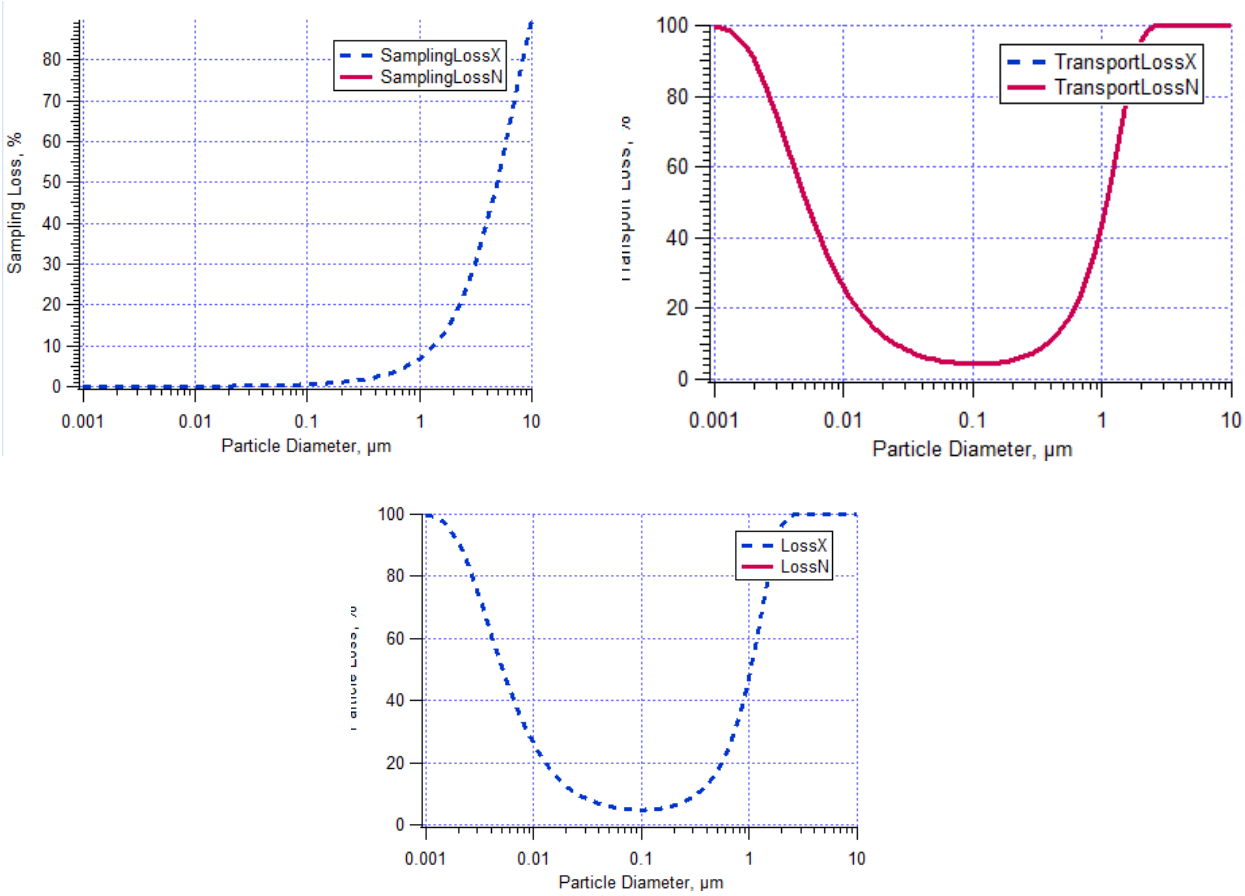

Figure 17 loss calculation Diameter, losses at inlet, losses in tubing, total losses. Assumed density 1.5 and spherical particles

4.0 RESULTS AND DISCUSSION

4.1 Metals Concentration in Atmospheric Aerosol in Lund

During the first measurement campaign in the city of Lund, 14 elements were used for analysis. Based on previous aerosol measurements, the elements normally present in atmospheric airborne particles and identified by XACT are S, Cl, K, Ca, Ti, V, Cr, Fe, Ni, Cu, Zn, Br, Sr, and Pb. Due to disruptions in the measurement setup at the IKDC laboratory, certain samples were never analyzed. Also, it was decided that elements should have been detected at least 50% of the time to be included in the calculation of average or median concentrations. The remaining 14 elements which occasionally contained zero values, were assigned a random value between zero and the detection limit from XACT manual, to come up with a more reliable estimate of the average mass concentration for the entire period.

Table 5 shows the average concentrations and standard deviations of the fine particles for the elements measured during the first measurement period at IKDC at the urban background Lund city station. These values are compared to measurements in Landskrona urban background station, “Stadshuset” in 1977, 1988, 2003, 2008, and 2017. Landskrona has situated 28 km to the northwest of Lund but with a smaller population of 34 000. The 2022 concentration

represents the average of 19 days from September 15 to October 3, at the IKDC at the urban background Lund city station. While the 2017 concentration represents the average of 36 measurement days from mid-February, at Stadshuset, 2008 concentrations are average concentrations measured during 5 weeks in the spring, and the 2003 concentrations are also average concentrations measured during 5 weeks in the spring. The 1988 concentrations are average concentrations measured during 4 weeks in winter and spring, and the 1977 concentrations are recalculated annual concentrations that were sampled over 16 days during a half-year period. (Kristensson, A.,2019 & Prosper, W. 2017 *).

Table 4 Average PM1 mass concentrations and standard deviations of elements which were above zero concentration values during at least 50 % of the time. Data on previous measurements in Landskrona urban background air at the city hall (Stadshuset) are included

Element	2022	SD (σ) 2022	2017	2008	2003	1988	1977
Al	-	-	40	10.4	50.4	-	-
Si	-	-	80	39.9	147	-	-
S	97.6	110.4	360	277.8	1241	1500	1800
Cl	22.6	40.3	720	0.2	162	24	160
K	18.0	13.9	69	29.9	144	79	150
Ca	3.9	6.0	44	30	102	47	200
Ti	0.7	1.6	0.97	2.65	7.8	4	22
V	0.2	0.4	1.5*	2.64	9.3	3	13
Cr	1.7	5.2	4.8	2.32	1.8	4.2	3.9
Fe	20.1	36.8	51	53.8	61.9	62	400
Ni	0.8	1.9	1.08	1.75	3.3	2	6.9
Cu	2.0	4.3	1.97	1.62	8	1.98	13
Zn	3.6	4.3	9.8	9.17	22.4	34	100
As	-	-	0.8*	0.2	3.9	-	-
Se	-	-	0.1*	0.13	-	-	-
Br	0.5	0.4	0.94	1.36	3.8	31	21
Sr	0.1	0.1	0.6*	0.1	0.4	-	-
Sn	-	-	0.3*	0.04	35.9	-	-
Pb	3.0	15.4	3.9	4.15	38.1	38	420

Examining the average concentrations further, it can be discovered that the concentration of most of the elements decreased compared to the previous measurements that took place in Landskrona (Stadshuset) in five different years. The only exceptions are Cu and Cl. Cl is higher than the 2008 measurements and that is basically due to an increased number of days with wind directions directly from the ocean. Increased wind speeds would also stimulate the production of sea spray and increase the concentration of measured Cl. The average Cu concentration is relatively high compared to the average concentrations in 2017, 2008, and 1988.

Sulfur, S, had the highest average concentration followed by chlorine (Table 5), (Figure 18), and its source can be explained by two categories: Particulate matter from combustion emissions sources or general pollution sources from long-range transport, and sea salt particles, as well as chemically converted dimethyl sulfide (DMS) emitted by sea surface (Veres, P. et al, 2020). For sulfur, there was a period from September 24th to 26th with rater stable concentrations

around 200 ng/m3 for almost three days. Chlorine also showed a stable concentration during that period with a concentration around 0.1 ng/m3 and both correlated, However, on October 1, sulfur marked the highest values at around 700 ng/m^3 while chlorine remained stable at 0.1 ng/m^3 concentration (Figure 18). Figure 19 shows that the air mass arrived from central Europe during this day and the preceding days explaining a high influence of polluted air from the south. Conversely, October 2 concentrations indicate high wind speeds and an ocean air mass origin pointing towards the dominant sea spray source when the sulfur concentrations dropped to around 100 ng/m3.

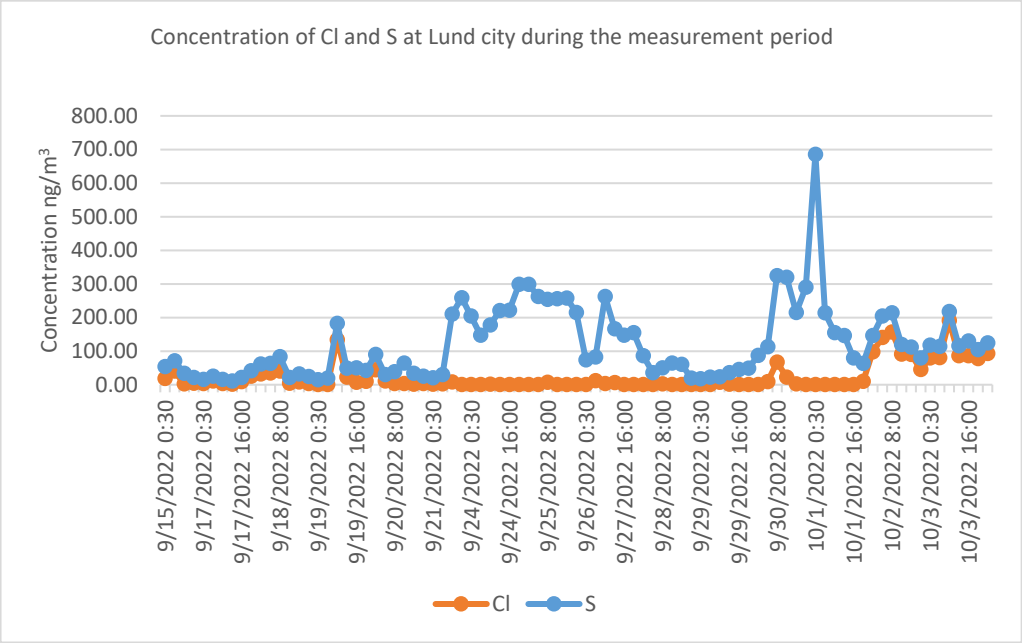

Figure 18 The concentration of sulfur and Chlorine at Lund Station during the first measurement period.

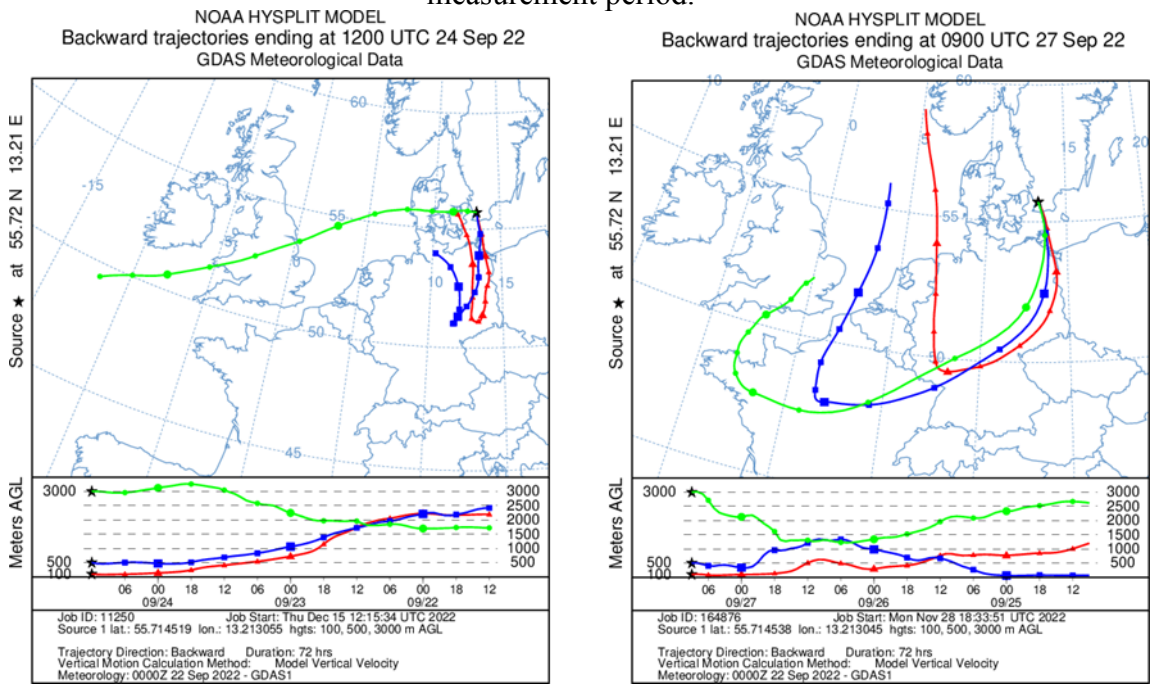

Figure 19 The trajectory plot for 100 m,500 m, and 3000 m ending at Lund (IKDC) on the 24, and 27 of September and the 1, 2 of October.

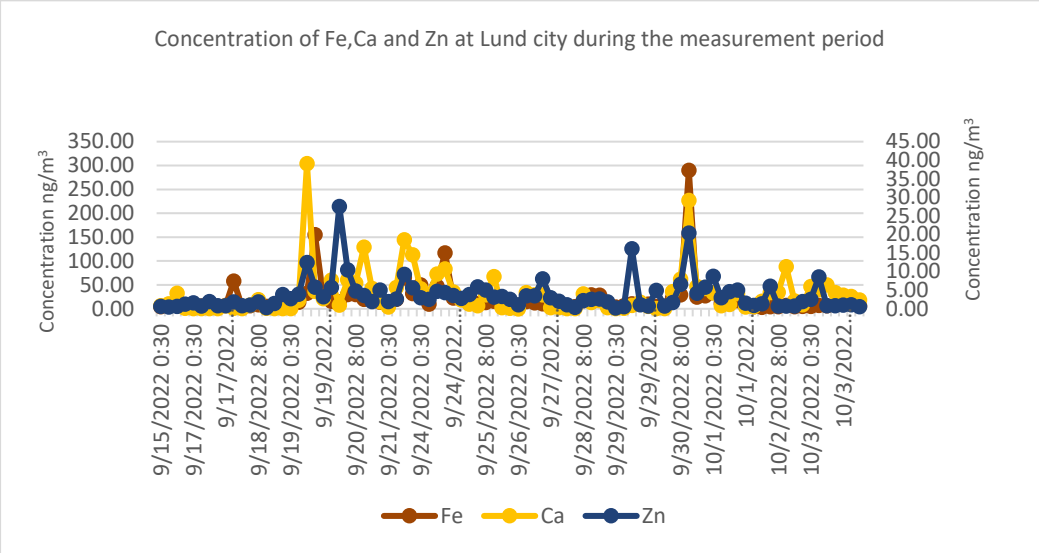

Figure 20 The concentration of Iron, Calcium, and Zinc at Lund Station during the first measurement period. (Fe, Primary Axis to the left, Ca and Zn Secondary Axis)

Figure 20 illustrates the concentrations of three different elements (Fe, Ca, and Zn). There are some peaks where elements go up together in some events, while during some periods it is obvious that for example, zinc has different sources, which are correlating with neither Ca nor Fe. Since Ca and Fe are normally associated with dust, and both are correlating more or less throughout the period (Table 6, correlation coefficient ~0.55), it is reasonable to assume Fe and Ca have a clear dust source. Zn correlates with these compounds (~0.45), and thereby also comes from this source, but not always. The additional Zn source is likely a Cu/Zn source of unclear origin that has been also identified during the previous Landskrona measurements (Kristensson et al., 2019). Figure 22 and Table 6 confirm that these correlate with a correlation coefficient of ~0.62.

However, Fe correlates best with Cr and Ni according to Table 6 and Figure 21. This is indicative of a presumed contribution of a fossil fuel combustion source, especially the combustion of heavy oil, which contains traces of Ni, Cr, and Fe. While the sulfur and Cl general long-range pollution source and sea spray particles show relatively stable concentrations over an extended period, the high metal concentrations are intermittent in behavior. The latter indicates local sources or near-regional sources. However, trajectories do not confirm differences in metal concentrations during these short periods, why this issue has to be investigated further.

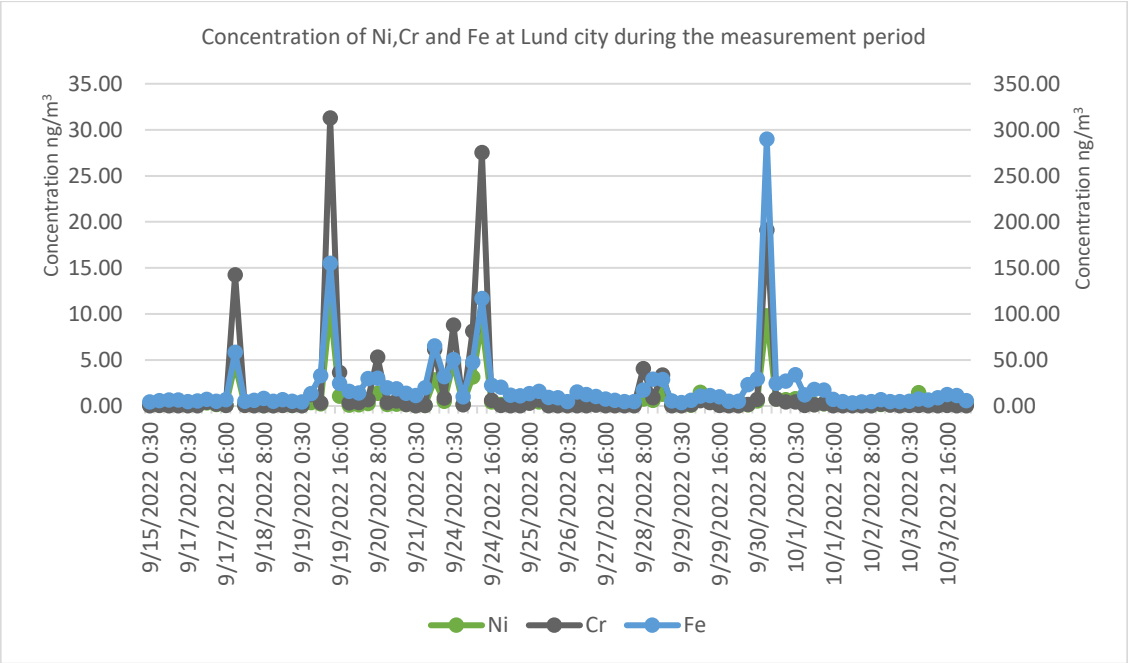

Figure 21 The concentration of Nickel, Chromium, and Iron at Lund Station during the first measurement period.

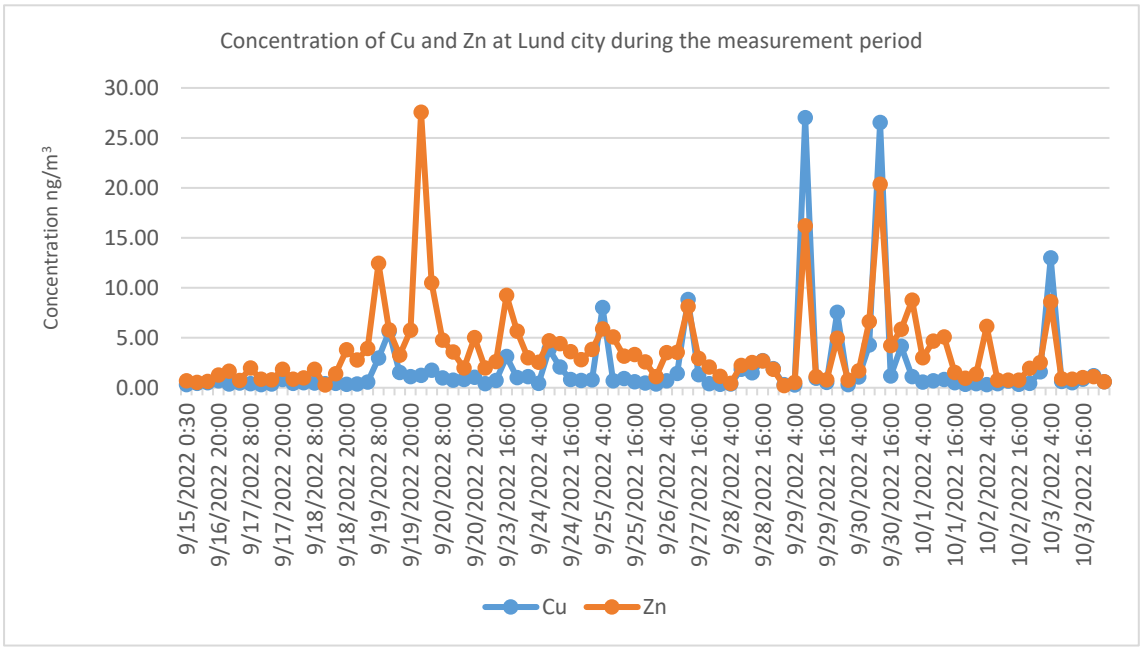

Figure 22 The concentration of Copper and Zinc at Lund Station during the first measurement period.

Table 5 Correlation matrix for the Lund station. Cell colors are attributed; accordingly, red, is the minimum point= -1, white midpoint = 0 and green is the maximum point = 1.

Element	*S*	*Cl*	*K*	*Ca*	*Ti*	*V*	*Cr*	*Fe*	*Ni*	*Cu*	*Zn*	*Br*	*Sr*	*Pb*
S	1													
Cl	-0.23558	1												
K	0.323772	-0.09057	1											
Ca	0.217992	0.277097	-0.00187	1										
Ti	0.105416	-0.11486	0.146277	0.391193	1									
V	0.610259	-0.02188	0.195571	0.11209	0.063969	1								
Cr	0.113619	-0.08056	0.01948	0.303301	0.250294	0.032664	1							
Fe	0.286878	-0.06991	0.054861	0.554765	0.330613	0.162622	0.816621	1						
Ni	0.192607	-0.05727	0.004369	0.366078	0.247256	0.131773	0.970499	0.891634	1					
Cu	0.135278	-0.00895	-0.07555	0.324716	0.092796	0.212168	0.301067	0.54935	0.460184	1				
Zn	0.27304	0.02301	0.469939	0.461888	0.300333	0.208743	0.229369	0.465706	0.327337	0.618572	1			
Br	0.911114	-0.18107	0.368965	0.298505	0.217917	0.609693	0.169518	0.296635	0.235616	0.076053	0.296921	1		
Sr	-0.00706	0.215922	-0.04166	0.231927	0.168351	0.023401	0.308986	0.313635	0.328079	0.176809	0.20753	0.049199	1	
Pb	0.020869	0.284809	0.029177	0.700055	0.070221	-0.01581	0.019691	0.148637	0.034661	0.110447	0.30478	0.023723	-0.0109	1

Element K has been associated with various sources in previous studies, for example, coal combustion and biomass combustion (Yu, J., et al., 2018). It has also been associated with markers from other sources such as Cl (from sea salt particles), Ca (from mineral dust particles), and S (from a general long-range transported fossil fuel combustion source, sea salt particles, and DMS oxidation).

Elements such as Ca, Fe, Cu, Zn, Ni, and Pb showed increases in some events, especially on September 19 and 30, which may indicate that the sources of pollution are closely related to all of these elements. It is also possible that some of these elements have a different source at the same time, which is more likely for Ni and Fe because the concentration values are relatively higher than the rest of the elements. The reasons for these high concentrations are unknown, and the trajectories do not indicate a specific source region. These may be erroneous data. A later comparison with PIXE filter samples might reveal this.

On one of these two days, September 19, the element arsenic (As) had a high concentration of about 1 ng/m3. The source could be related to coal combustion, since the concentration of Pb also showed a very high value of about 140 ng/m^3 in this sample, both As and Pb are used as markers for coal burning. (Yu, J., et al. 2018). Probably, industrial emissions and combustion of fossil fuels have some relationship during this occasion, since Fe, Cu, and Zn also showed high concentrations in the same sampling period, which all of them are associated with industrial and fossil fuels emission sources.

Also, As can be produced in the smelting furnace process. (Duan, J., & Tan, J. 2013). What is interesting, is that the air is stemming from the northern part of Sweden (Figure 23), which could be a reason for the high Pb concentration, since the Boliden Bergsoee lead recycling factory is north of Lund. However, it should not be the reason for high As values, since previous Landskrona measurements have not revealed high As concentrations (Norlin, M., & Savér, L. 2022). Moreover, steel, plastics pigments production, contaminated soils, and other particles that re-enter the atmosphere could

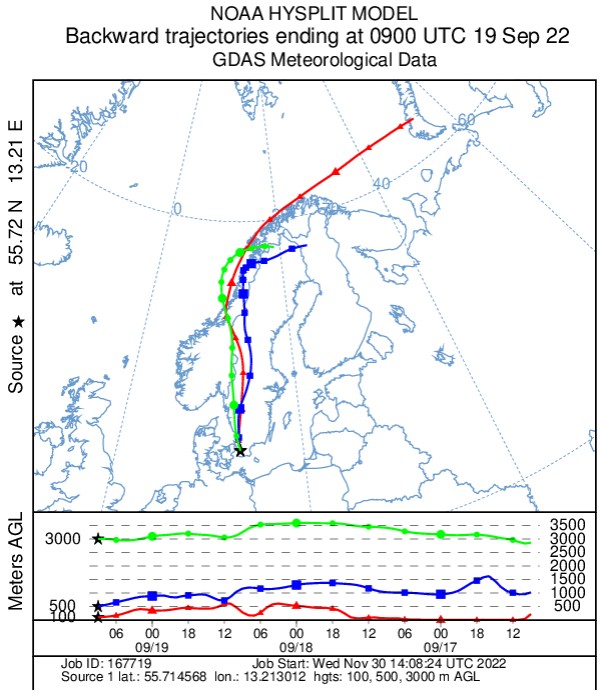

Figure 23 The trajectory plot for 100 m,500 m and 3000 m

contribute to the lead concentration. (Duan, J., & Tan, J. 2013). S in the data from Lund correlates to some extent with, for example, K, V, and Br (Table 6).

According to Kristensson et al. (2019), a source transported over long distances has been identified that contains mainly V, Ni, and S in the fine fraction. This comes from the combustion of heavy fuel oil from other countries and from local and regional ship emissions associated with high-sulfur fuel and lubricating oil containing the metals V and Ni. In part, it is also a general long-range source, containing sulfur dioxide emissions from industry and power generation, as well as emissions from sea spray resulting from wind-driven production of suspended particles during wave breaking, containing Cl, Br, Sr, and S. This can be supported by the air trajectories that mostly came from Germany and Poland for the concentration associated with sources that are not related to sea spray emissions, such as industrial emissions and combustion emissions sources, while in the events when the sea spray emissions from the North Sea contributing to the concentration, we see both Cl and S increase together, as in 19,30 of September and 02 of October (Figure 18).

Elements such as Ca, Fe, Cu, Zn, Ni, and Pb as mentioned above were found to be related to each other during the increasing concentration events, which makes it likely that they at least partly originated from a soil dust source, as these elements are associated with the Earth's crust (Kristensson et al. 2019). It is also possible that some of these elements, such as Ni, are derived from the long-range transport of fossil combustion particles, as fossil oil often contains Ni. (Kristensson et al. 2019). Ni is also associated with Vehicle tailpipe emissions from a road traffic source and coal and oil combustion sources (Maciejczyk, P., et al 2021). Cu/Zn concentrations are more likely to be generated from different sources as we can see in the graph Figure 22, both elements are correlated in all the measurement periods except on 20 of September where Zn increased and marked the highest value, while Cu did not increase (Figure 22). The analysis of metal concentrations and quantification of their source contributions will be evaluated in the future using source/receptor modeling.

Strontium marked the lowest average concentration at 0.1 ng/m3 among the 14 elements presented in Table 5. Sr occurs naturally in the Earth's crust and is released into the atmosphere through natural processes such as wind dust resuspension, also Sr can be associated with sea spray (Capo et al. 1998). Also, it has the potential to be associated with stack emissions from coal-burning plants and be transported over longer distances. (Watts, P., & Howe, P. 2010). Dust from the parking lot or nearby streets is a probable candidate, although this is not further investigated here.

4.2 METALS CONCENTRATION IN ATMOSPHERIC AEROSOL IN HYLTEMOSSA

In the second measurement location Hyltemossa, 17 elements were used for analysis S, Cl, K, Ca, Ti, V, Cr, Mn, Fe, Ni, Cu, Zn, Se, Br, Rb, Sr and Pb. The same role of 50% detection of elements has been used for Hyltemossa data to be included in the calculation of average or median concentrations. The remaining values among the 17 elements that showed zero values, were assigned a random value between zero and the detection limit from XACT manual, to come up with a more reliable estimate of the average mass concentration for the entire period.

Table 7 shows the average concentrations and standard deviations of the PM10 particles for the elements measured during the second measurement campaign at Hyltemossa rural background station. These values are compared to measurements in Vavihill rural background station during 2000. Vavihill has situated about 20 km to the west-south-west of Hyltemossa. The 2022 concentration represents the average of one-month data from October 19 to November 19, at the Hyltemossa rural background station, while the - 2000 concentrations at Vavihill were carried out for almost six months, from January to May (Kristensson et al. 2019).

Table 7: Average PM10 mass concentration values and standard deviations of elements, which were above zero concentration values during at least 50 % of the time Data on previous measurements in Vavihill rural station are included for comparison. Concentration in nanogram per cubic meter (ng/m^3).

Element	Hyltemossa 2022	SD (σ) 2022	*Vavihill* 2000
S	337.67	315.84	479
Cl	395.43	569.5	575
K	68.24	35	87.5
Ca	42.23	34.83	77.4
Ti	2	2.95	5.1
V	0.58	0.57	0.4
Cr	1.97	22.51	1.3
Mn	0.9	1.22	2.6
Fe	50.48	53.44	62.5
Ni	0.66	4.3	0.2
Cu	1.39	0.99	1.2
Zn	7.53	7.74	7.9
Se	0.21	0.21	0.5
Br	2.22	1.46	5.6
Rb	0.16	0.17	-
Sr	0.56	0.47	0.4
Pb	5	6.62	4.1

Examining the average concentrations further, it can be discovered that the concentration of most of the elements decreased compared to the previous measurements that took place in Vavihill 2000. Only 6 elements showed a little higher concentration than the 2000 measurements, such as Vanadium (V), chromium (Cr), nickel (Ni), copper (Cu), Strontium (Sr), and Lead (Pb). A possible Vanadium and Nickel source is fossil fuel ship emissions. The Vanadium to Nickel ratio has decreased from about 2 to about 1, which could be an indication of the fuel switch in the shipping sector from sulfur-rich heavy fuel oil towards lower sulfur-containing heavy fuel oil or marine diesel or gasoline oil (Yu et al.,2021). In general, there were frequent winds from the south in the Hyltemossa measurement period, why these elements also indicate we influence ship traffic and continental pollution sources.

Chlorine showed fluctuations in concentration most of the time except five days in the beginning and two days in the mid-period and at the very end, where the concentration was remaining at low levels. The higher concentration above 2000 ng/m^3 was mainly contributed by the sea spray from the North Sea during all the higher-level

concentration values as can be seen in Figure 25, which was not the case for sulfur concentration during those periods. Sulfur, S, had the four outliers as seen in Figure 24, in all four occasions the air mass arrived from central Europe during those days explaining a high influence of polluted air from the south as Figure 26 indicated. That can support what has been said by Veres, P. et al, (2020) "Particulate matter can be from combustion emissions sources or general pollution sources from long-range transport". Furthermore Sulfur (S) in the combustion source was mainly due to the condensation of sulphuric acid onto nanoparticles during long-range transport. (Prosper, W. 2017).

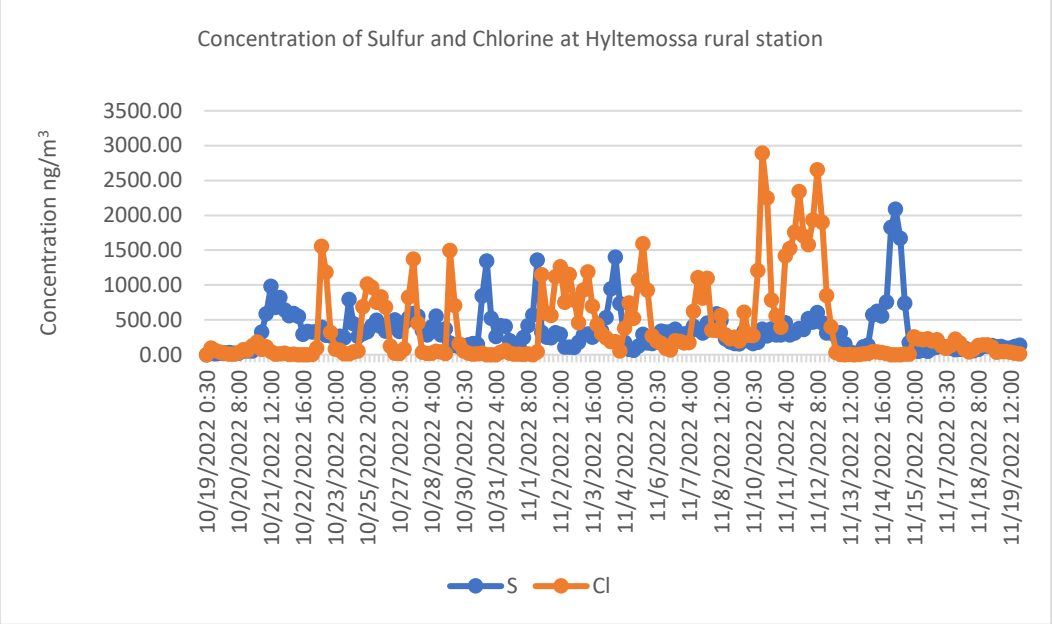

Figure 24 The concentration of Sulfur and Chlorine at Hyltemossa rural Station during the second measurement period.

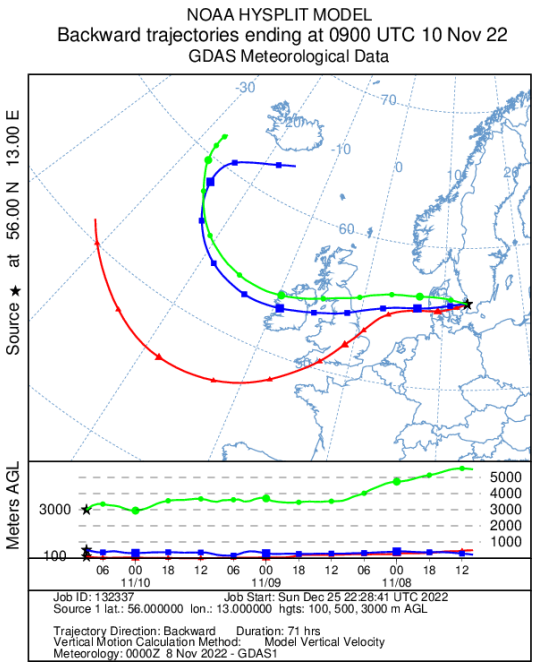

Figure 25 The trajectory plot for 100 m,500 m, and 3000 m

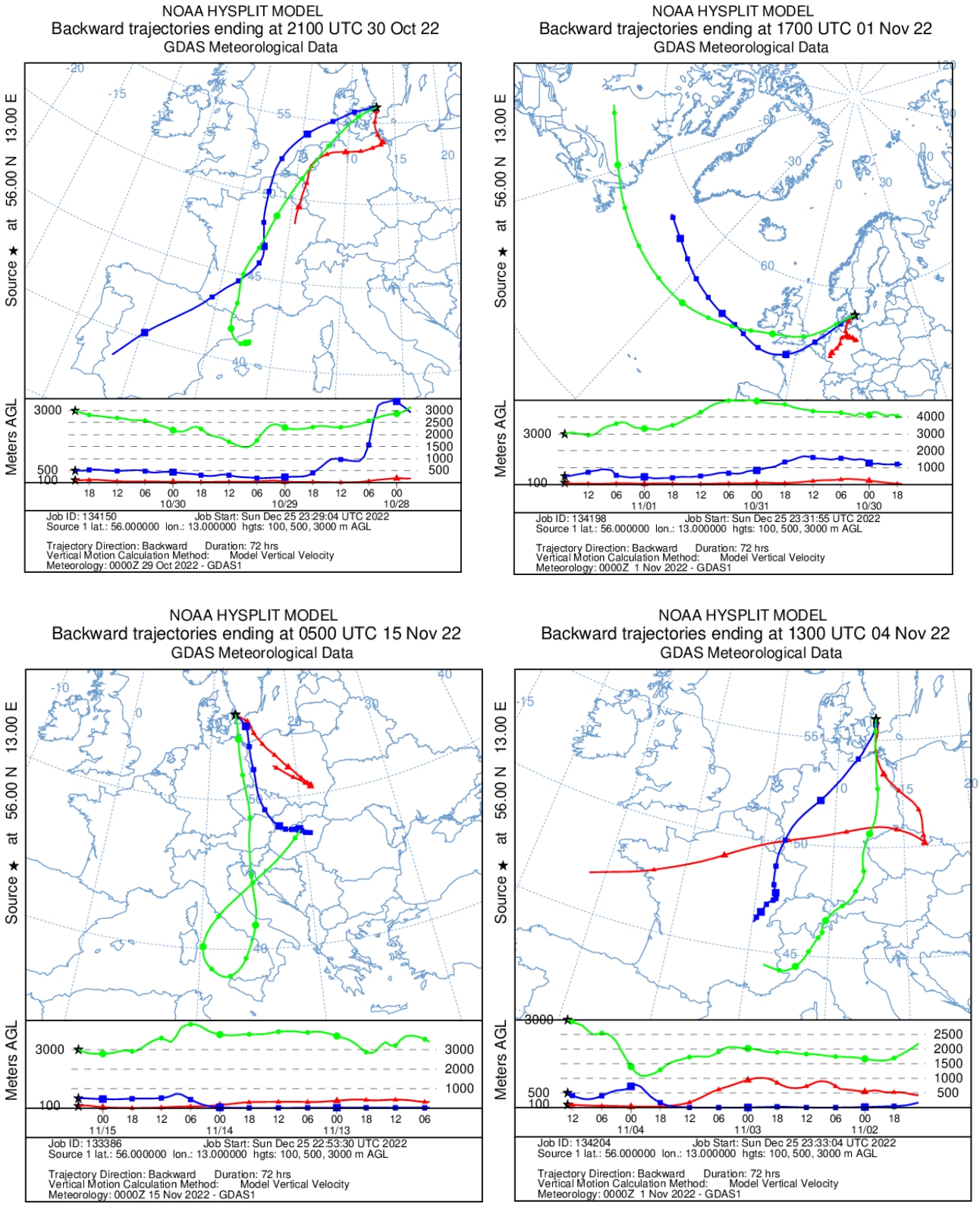

Figure 26 The trajectory plot for 100 m,500 m and 3000 m ending at Hyltemossa on 30 of October,1,4 and 15.

Potassium was the third highest concentration element with an average concentration of about 70 ng/m3. Element K has as previously mentioned, been associated with various sources in previous studies, for example, dust, coal, or biomass combustion (Yu, J., et al. 2018). However, in this case it is more likely that domestic wood combustion is the main source of the high K concentration in this study, since K concentrations showed higher values at night, when more intense domestic wood combustion activity is expected. Cu and Zn decreased and increased simultaneously most of the time, which indicates that their sources are similar, which was also the case for the Lund data.

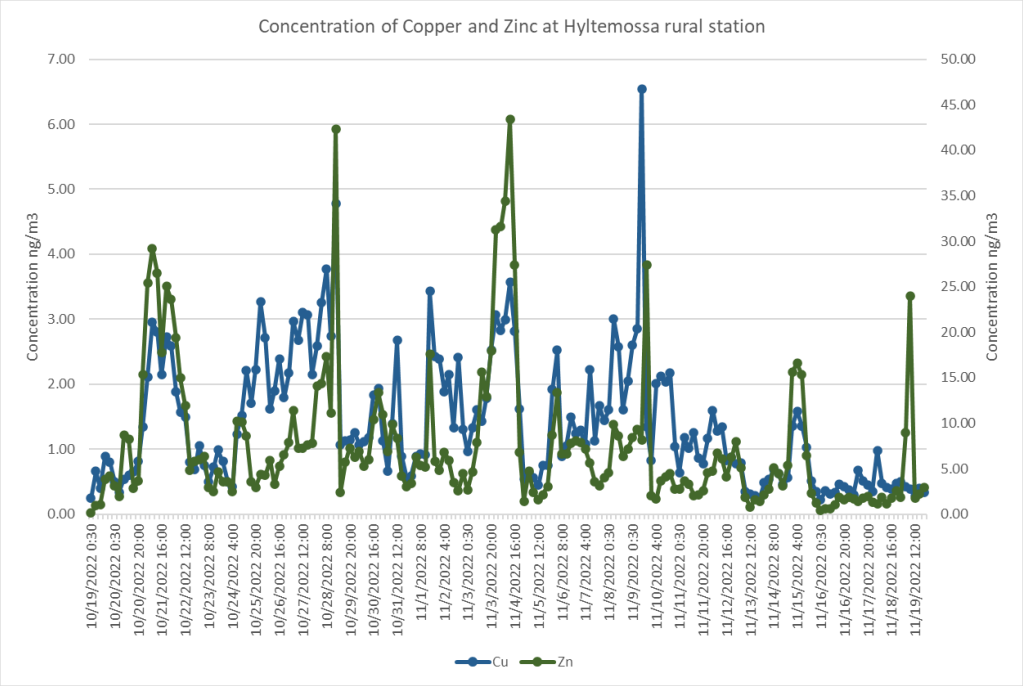

Figure 27 The concentration of Cu, and Zn at Hyltemossa rural Station. Zn on the right Axis.

Ca correlated with Fe throughout the period (Figure 28), which indicates a mineral dust source. It also correlated with Zn, which indicates that the Cu/Zn source is partly emanating from mineral dust.

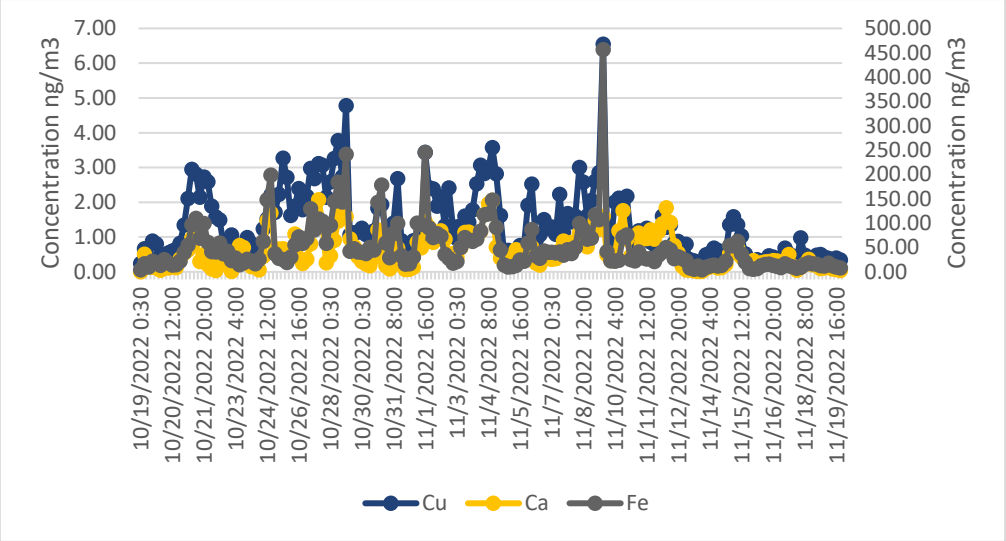

Figure 28: The concentration of Cu, Ca, and Fe at Hyltemossa Rural Station. Fe on the right Axis.

Arsenic showed a relatively high concentration for more than 30% of the samples, the highest value was about 2 ng/m^3 on the 22 of October during the night as can be seen in Figure 29. There was a correlation between As and Zn (around 0.7). Also, Pb increased at the same time as As on one occasion., the source could be related to industrial emissions since As is likely from coal combustion transported over longer distances from central Europe Figures 26 and 30 (Yu, J., et al. 2018 & Maciejczyk, P., et al 2021).

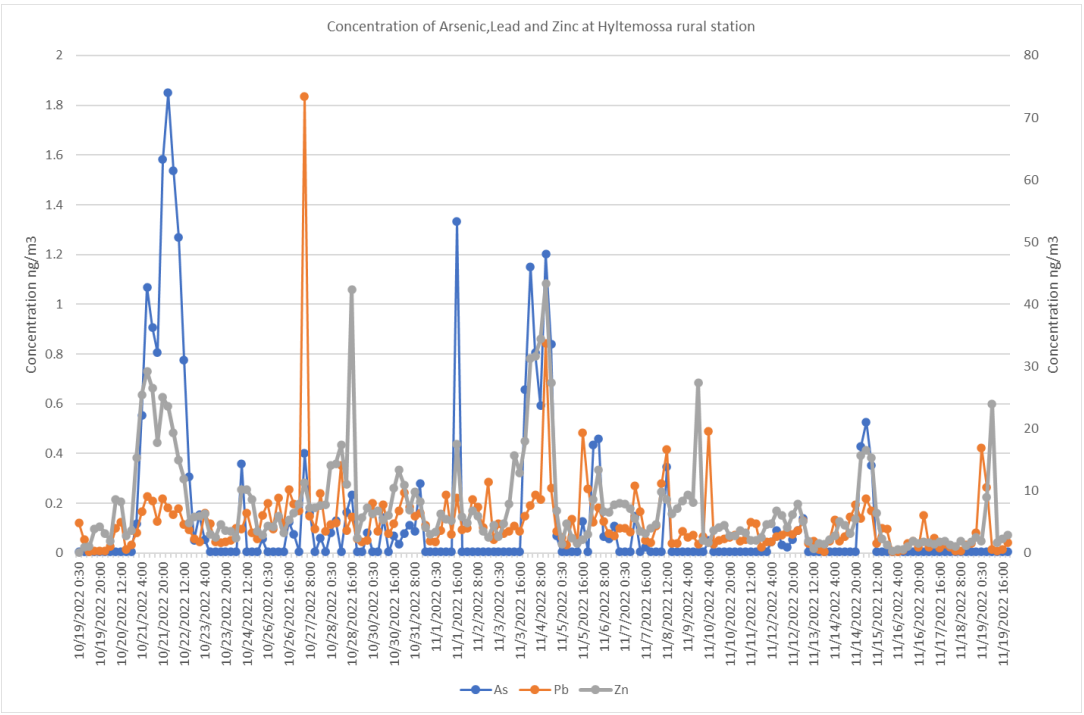

Figure 29: The concentration of As, Pb, and Zn at Hyltemossa rural Station. Pb and Zn on the right Axis.

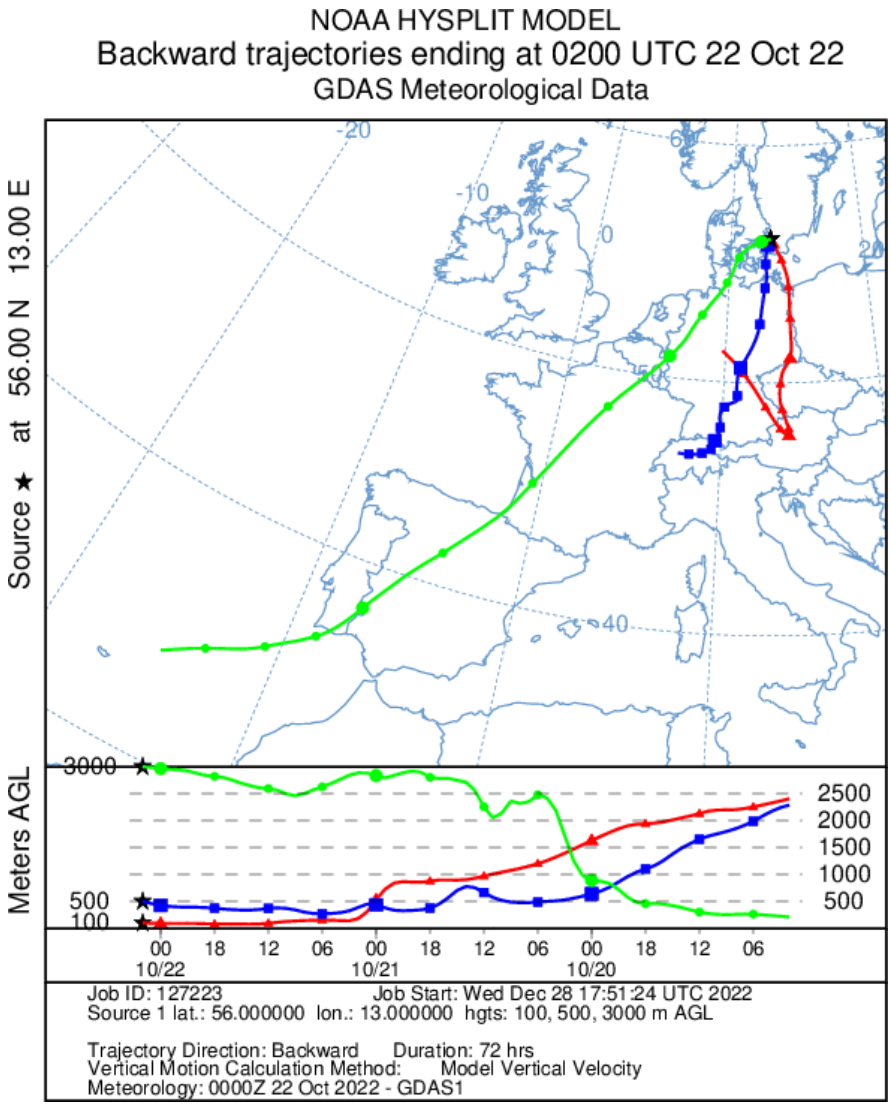

Figure 30: The trajectory plot for 100 m,500 m and 3000 m ending at Hyltemossa on 22 of October.

Table 8: Correlation matrix for the rural background station Hyltemossa. Cell colors are attributed; accordingly, red, is the minimum point= -1(strong negative relationship), white midpoint = 0 (no relationship) and green is the maximum point = 1 (strong positive relationship). Two values where Cr and Ni showed abnormally high concentrations were removed during correlation coefficient calculation to maintain a reasonable relationship between the elements.

	S	*Cl*	*K*	*Ca*	*Ti*	*V*	*Cr*	*Mn*	*Fe*	*Ni*	*Cu*	*Zn*	*Se*	*Br*	*Rb*	*Sr*	*Pb*
S	1.00000																
Cl	-0.01682	1.00000															
K	0.53568	0.06349	1.00000														
Ca	0.37786	0.50934	0.50937	1.00000													
Ti	0.44630	-0.18706	0.58288	0.55122	1.00000												
V	0.21619	-0.10140	0.51908	0.27686	0.49522	1.00000											
Cr	0.00302	0.03208	0.02936	0.16486	0.04601	0.01642	1.00000										
Mn	0.34356	-0.08964	0.51477	0.57715	0.59757	0.35651	0.71005	1.00000									
Fe	0.40698	-0.05925	0.58385	0.66562	0.76638	0.47579	0.57942	0.94494	1.00000								
Ni	0.01158	0.02889	0.05105	0.17297	0.05816	0.06001	0.36738	0.44244	0.59297	1.00000							
Cu	0.41242	0.10228	0.66573	0.69456	0.54831	0.36658	0.40159	0.81040	0.83292	0.41373	1.00000						
Zn	0.52211	-0.20455	0.58255	0.40924	0.50670	0.18958	0.00902	0.53554	0.52179	0.01524	0.60791	1.00000					
Se	0.63346	0.01661	0.75949	0.51020	0.51186	0.33753	0.04863	0.56721	0.58435	0.06212	0.69658	0.76382	1.00000				
Br	0.49766	0.60750	0.56083	0.71451	0.21433	0.24702	0.05876	0.30378	0.36553	0.07287	0.53399	0.34444	0.56013	1.00000			
Rb	0.20390	-0.35239	0.66846	0.06199	0.47333	0.36499	-0.00675	0.33461	0.34473	0.00516	0.26535	0.36925	0.39359	0.02758	1.00000		
Sr	0.25792	0.75555	0.43036	0.84119	0.32306	0.17123	0.06075	0.28655	0.38154	0.06687	0.50102	0.15264	0.34693	0.76866	-0.06667	1.00000	
Pb	0.28216	-0.06042	0.29327	0.20849	0.18521	0.22531	-0.02310	0.24326	0.27389	-0.01326	0.36200	0.31283	0.32383	0.15389	0.00000	0.04848	1

Conclusion

Elevated concentrations of Cu, Ni, Cr, and Pb were measured several times in both the city of Lund and Hyltemossa. Compared to previous campaigns for urban emissions, there is a clear downward trend in average element concentrations. In contrast, compared to the 2008 average concentrations for Cl and Cu from 2017, 2008, and 1988, there is an increase, but this is likely due to more winds from ocean areas in this study giving relatively higher contribution from the sea spray source. For the rural background measurements in Hyltemossa, V, Cr, Ni, Cu, Sr, and Pb were higher on average than for the Vavihill rural measurements during 2000. This was likely due to more frequent winds from continental polluted regions in this study.

A few samples with high concentrations have a significant impact on the average concentrations of heavy metals. The elevated concentrations did not exceed the environmental quality standards' annual average limit, which does not mean that these are not unhealthy. From the trajectories, it appears that the heavy metal concentration often originates from long-range transboundary sources in Central Europe. There should certainly be a local or near-regional source origin of several of the elements measured in Lund and Hyltemossa as well, but this could not be proven in this study, besides a wood combustion source, which is likely local or near-regional by nature.

Although, the concentrations in Lund and Hyltemossa are not above regulative limits, decreases in anthropogenic elements should have a positive effect on human health. Nevertheless, the elements measured in Lund and Hyltemossa are very useful as source markers in source/receptor modeling attributing PM mass concentrations to specific anthropogenic and natural sources. PM mass concentrations in contrast to elements are proven to have adverse health effects in southern Sweden, and therefore it is crucial to measure these elemental source markers for an effective abatement strategy for air pollution.

REFERENCES

Amann, M., Kiesewetter, G., Schöpp, W., Klimont, Z., Winiwarter, W., Cofala, J., ... & Pavarini, C. (2020). Reducing global air pollution: the scope for further policy interventions. Philosophical Transactions of the Royal Society A, 378(2183), 20190331.

Ambient (outdoor) air pollution. World Health Organization. https://www.who.int/news-room/fact-sheets/detail/ambient-(outdoor)-air-quality-and-health (2022).

Ansmann, A., B¨osenberg, J., Chaikovsky, A., Comer´on, A., Eckhardt,S. and co-authors. 2003. Long-range transport of Saharan dust to northern Europe: the 11–16 October 2001 outbreak observed withEARLINET.J. Geophys.https://doi.org/10.1029/2003JD003757

ATSDR. Toxicological profile for copper. US Department of health and Human services. 2022: available at https://www.atsdr.cdc.gov/toxprofiles/tp132.pdf

Bond, T. C., Doherty, S. J., Fahey, D. W., Forster, P. M., Berntsen, T., DeAngelo, B. J., ... & Zender, C. S. (2013). Bounding the role of black carbon in the climate system: A scientific assessment. Journal of geophysical research: Atmospheres, 118(11), 5380-5552.

Boucher, O. (2015). Atmospheric aerosols. In Atmospheric Aerosols (pp. 9-24). Springer, Dordrecht.

Capulli, D., & Oliveira, E. N. D. M. N. (2014). Air Cleaner to Make Up Air in Adverse Thermal and Environmental Conditions.

Chen, Z., Meng, H., Xing, G., Chen, C., Zhao, Y., Jia, G., ... & Wan, L. (2006). Acute toxicological effects of copper nanoparticles in vivo. Toxicology letters, 163(2), 109-120.

Connan, O., Maro, D., Hébert, D., Roupsard, P., Goujon, R., Letellier, B., & Le Cavelier, S. (2013). Wet and dry deposition of particles associated metals (Cd, Pb, Zn, Ni, Hg) in a rural wetland site, Marais Vernier, France. Atmospheric Environment, 67, 394-403.

Corbin, J. C., Mensah, A. A., Pieber, S. M., Orasche, J., Michalke, B., Zanatta, M., ... & Gysel, M. (2018). Trace metals in soot and PM2. 5 from heavy-fuel-oil combustion in a marine engine. Environmental science & technology, 52(11), 6714-6722.

Dahneke, B. (1983). Simple kinetic theory of Brownian diffusion in vapors and aerosols. In *Theory of dispersed multiphase flow* (pp. 97-133). Academic Press.

Demayo, A., Taylor, M. C., Taylor, K. W., Hodson, P. V., & Hammond, P. B. (1982). Toxic effects of lead and lead compounds on human health, aquatic life, wildlife plants, and livestock. Critical reviews in environmental science and technology, 12(4), 257-305.

Duan, J., & Tan, J. (2013). Atmospheric heavy metals and arsenic in China: situation, sources and control policies. Atmospheric Environment, 74, 93-101.

Duhanyan, N., & Roustan, Y. (2011). Below-cloud scavenging by rain of atmospheric gases and particulates. Atmospheric Environment, 45(39), 7201-7217.

EEA. Agency, E. E. (2021, December 3). Air Quality Standards. European Environment Agency. Retrieved October 18, 2022, from https://www.eea.europa.eu/themes/air/air-quality-concentrations/air-quality-standards

EEA. Agency, E. E. (2022, September 19). Europe's Air Quality Status 2022. European Environment Agency. Retrieved October 18, 2022, from https://www.eea.europa.eu//publications/status-of-air-quality-in-Europe-2022

Fennelly, M. J., Sewell, G., Prentice, M. B., O'Connor, D. J., & Sodeau, J. R. (2017). The use of real-time fluorescence instrumentation to monitor ambient primary biological aerosol particles (PBAP). Atmosphere, 9(1), 1.

Flemming, C. A., & Trevors, J. T. (1989). Copper toxicity and chemistry in the environment: a review. Water, air, and soil pollution, 44(1), 143-158.

Fuller, R., Landrigan, P. J., Balakrishnan, K., Bathan, G., Bose-O'Reilly, S., Brauer, M., ... & Yan, C. (2022). Pollution and health: a progress update. The Lancet Planetary Health.

Furger, M., Minguillón, M. C., Yadav, V., Slowik, J. G., Hüglin, C., Fröhlich, R., ... & Prévôt, A. S. (2017). Elemental composition of ambient aerosols measured with high temporal resolution using an online XRF spectrometer. Atmospheric Measurement Techniques, 10(6), 2061-2076.

Glasius, M., & Goldstein, A. H. (2016). Recent discoveries and future challenges in atmospheric organic chemistry.

Grahame, T. J., Klemm, R., & Schlesinger, R. B. (2014). Public health and components of particulate matter: the changing assessment of black carbon. Journal of the Air & Waste Management Association, 64(6), 620-660.

Greeley, R., Iversen, J., Leach, R., Marshall, J., White, B., & Williams, S. (1984). Windblown sand on Venus: Preliminary results of laboratory simulations. Icarus, 57(1), 112-124.

Griffin, D. W. (2007). Atmospheric movement of microorganisms in clouds of desert dust and implications for human health. Clinical microbiology reviews, 20(3), 459-477.

Grönqvist, H., Nilsson, J. P., & Robling, P. O. (2017). Early lead exposure and outcomes in adulthood (No. 2017: 4). Working Paper.

Hakkarainen, H., Salo, L., Mikkonen, S., Saarikoski, S., Aurela, M., Teinilä, K., ... & Jalava, P. I. (2022). Black carbon toxicity dependence on particle coating: Measurements with a novel cell exposure method. Science of The Total Environment, 156543.

Harbison, R. D., Bourgeois, M. M., & Johnson, G. T. (2015). Hamilton and hardy's industrial toxicology. John Wiley & Sons.

Harrison, R. M., Van Vu, T., Jafar, H., & Shi, Z. (2021). More mileage in reducing urban air pollution from road traffic. Environment International, 149, 106329.

Heat, C. (2016). Residential Wood Burning: Environmental Impact and Sustainable solutions. Deutsche Umwelthilfe and The Danish Ecological Council.

Hinckley, EL.S., Crawford, J.T., Fakhraei, H. et al. A shift in sulfur-cycle manipulation from atmospheric emissions to agricultural additions. Nat. Geosci. 13, 597–604 (2020). https://doi.org/10.1038/s41561-020-0620-3

Hinds, W. C., & Zhu, Y. (2022). Aerosol technology: properties, behavior, and measurement of airborne particles. John Wiley & Sons.

Huskin Okinedo, P. (2020). Comparison of soil CO2 efflux between different surface covers on a clear-cut and forest stand in southern Sweden, Hyltemossa. Student thesis series INES.

Hugony, F., Ozgen, S., Morreale, C., Signorini, S., Cernuschi, S., Maggioni, A., ... & Ripamonti, G. (2012). Nanoparticles size distribution in wood combustion. In 16th ETH-Conference on Combustion Generated Nanoparticles (pp. 1-5).

Jacobson, M. Z., & Turco, R. P. (1995). Simulating condensational growth, evaporation, and coagulation of aerosols using a combined moving and stationary size grid. *Aerosol science and technology*, *22*(1), 73-92.

Johansson, S. A. (1989). PIXE: a novel technique for elemental analysis. Endeavour, 13(2), 48-53.

Juginović, A., Vuković, M., Aranza, I., & Biloš, V. (2021). Health impacts of air pollution exposure from 1990 to 2019 in 43 European countries. Scientific reports, 11(1), 1-15.

Kabir, M. H. (2007). Particle induced X-ray emission (PIXE) setup and quantitative elemental analysis.

Kelly, F. J., & Fussell, J. C. (2020). Toxicity of airborne particles—established evidence, knowledge gaps and emerging areas of importance. Philosophical Transactions of the Royal Society A, 378(2183), 20190322.

Kolb, C. E., & Worsnop, D. R. (2012). Chemistry and composition of atmospheric aerosol particles. Annual review of physical chemistry, 63, 471-491.

Kristensson, A. (2005). Aerosol Particle Sources Affecting the Swedish Air Quality at Urban and Rural Level.

Kristensson, A., Prosper, W., Pallon, J., Feuk, E., Alikioti, D., & Nilsson, P. (2019). Metaller i luftburna partiklar i Landskrona 2017. LTH, Avdelningen för kärnfysik. Lunds Universitet

Kristensson, A., Prosper, W., Pallon, J., Feuk, E., Alikioti, D., & Nilsson, P. (2019). Metals in airborne particles in Landskrona 2017.

Kocbach, A., Johansen, B. V., Schwarze, P. E., & Namork, E. (2005). Analytical electron microscopy of combustion particles: a comparison of vehicle exhaust and residential wood smoke. Science of the total environment, 346(1-3), 231-243.

Kulmala, M., Kontkanen, J., Junninen, H., Lehtipalo, K., Manninen, H. E., Nieminen, T., ... & Worsnop, D. R. (2013). Direct observations of atmospheric aerosol nucleation. Science, 339(6122), 943-946.

Kumar Das, S., singh Grewal, A., & Banerjee, M. (2011). A brief review: Heavy metal and their analysis. Organization, 11(1), 003.

Lagzi, I., Mészáros, R., Gelybo, G., & Leelossy, A. (2013). Atmospheric chemistry.

Leelőssy, Á., Molnár, F., Izsák, F., Havasi, Á., Lagzi, I., & Mészáros, R. (2014). Dispersion modeling of air pollutants in the atmosphere: a review. *Open Geosciences*, *6*(3), 257-278.

Lelieveld, J., Klingmüller, K., Pozzer, A., Burnett, R. T., Haines, A., & Ramanathan, V. (2019). Effects of fossil fuel and total anthropogenic emission removal on public health and climate. Proceedings of the National Academy of Sciences, 116(15), 7192-7197.

Lewis, E. R., Lewis, R., & Schwartz, S. E. (2004). Sea salt aerosol production: mechanisms, methods, measurements, and models (Vol. 152). American geophysical union.

Liu, D., He, C., Schwarz, J. P., & Wang, X. (2020). Lifecycle of light-absorbing carbonaceous aerosols in the atmosphere. NPJ climate and atmospheric science, 3(1), 1-18.

Liu, Y., Zheng, M., Yu, M., Cai, X., Du, H., Li, J., Zhou, T., Yan, C., Wang, X., Shi, Z., Harrison, R. M., Zhang, Q., and He, K.: High-time-resolution source apportionment of PM2.5 in Beijing with multiple models, Atmos. Chem. Phys., 19, 6595–6609, https://doi.org/10.5194/acp-19-6595-2019, 2019.

Maciejczyk, P., Chen, L. C., & Thurston, G. (2021). The role of fossil fuel combustion metals in PM2. 5 air pollution health associations. Atmosphere, 12(9), 1086.

Mallone, S., Stafoggia, M., Faustini, A., Gobbi, G. P., Marconi, A., & Forastiere, F. (2011). Saharan dust and associations between particulate matter and daily mortality in Rome, Italy. Environmental health perspectives, 119(10), 1409-1414.)

Malmqvist, E., Liew, Z., Källén, K., Rignell-Hydbom, A., Rittner, R., Rylander, L., & Ritz, B. (2017). Fetal growth and air pollution-a study on ultrasound and birth measures. Environmental research, 152, 73-80.

Mariet, A. S., Mauny, F., Pujol, S., Thiriez, G., Sagot, P., Riethmuller, D., ... & Bernard, N. (2018). Multiple pregnancies and air pollution in moderately polluted cities: Is there an association between air pollution and fetal growth? Environment international, 121, 890-897.

Mariraj Mohan, S. (2016). An overview of particulate dry deposition: measuring methods, deposition velocity and controlling factors. International journal of environmental science and technology, 13(1), 387-402.

MARTIN, A. R., KRISTENSSON, A., & JOHNSON, M. S. The Aerosol-Chase Project.(2021)

Merikanto, J., Spracklen, D. V., Mann, G. W., Pickering, S. J., & Carslaw, K. S. (2009). Impact of nucleation on global CCN. *Atmospheric Chemistry and Physics*, *9*(21), 8601-8616.

Miller, R. L., Cakmur, R. V., Perlwitz, J., Geogdzhayev, I. V., Ginoux, P., Koch, D., ... & Tegen, I. (2006). Mineral dust aerosols in the NASA Goddard Institute for Space Sciences ModelE atmospheric general circulation model. Journal of Geophysical Research: Atmospheres, 111(D6).

Monahan, E. C., Fairall, C. W., Davidson, K. L., & Boyle, P. J. (1983). Observed inter-relations between 10m winds, ocean whitecaps and marine aerosols. Quarterly Journal of the Royal Meteorological Society, 109(460), 379-392.

Molnar, P., Gustafson, P., Johannesson, S., Boman, J., Barregård, L., & Sällsten, G. (2005). Domestic wood burning and PM2. 5 trace elements: Personal exposures, indoor and outdoor levels. Atmospheric Environment, 39(14), 2643-2653.

Norlin, M., & Savér, L. (2022) Diffuse dust at Boliden Bergsöe investigated through X-ray Fluorescence Spectroscopy.

Olszowski, T., & Bożym, M. (2014). Pilot study on using an alternative method of estimating emission of heavy metals from wood combustion. Atmospheric Environment, 94, 22-27.

Park, S. S., Cho, S. Y., Jo, M. R., Gong, B. J., Park, J. S., & Lee, S. J. (2014). Field evaluation of a near–real time elemental monitor and identification of element sources observed at an air monitoring supersite in Korea. Atmospheric Pollution Research, 5(1), 119-128.

Pettibone, A. J. (2009). Toward a better understanding of new particle formation (Doctoral dissertation, University of Iowa).

Perera, F. (2018). Pollution from fossil-fuel combustion is the leading environmental threat to global pediatric health and equity: Solutions exist. International journal of environmental research and public health, 15(1), 16.

Pilla, F., & Broderick, B. (2015). A GIS model for personal exposure to PM10 for Dublin commuters. Sustainable Cities and Society, 15, 1-10.

Prosper, W. (2017). The Metal Content in Airborne Particles in Landskrona.

Renzi, M., Stafoggia, M., Cernigliaro, A., Calzolari, R., Madonia, G., Scondotto, S., & Forastiere, F. (2017). Health effects of Saharan dust in Sicily Region (Southern Italy). Epidemiologia e Prevenzione, 41(1), 46-53.

Rittner, R., Flanagan, E., Oudin, A., & Malmqvist, E. (2020). Health impacts from ambient particle exposure in Southern Sweden. International journal of environmental research and public health, 17(14), 5064.

Ruijgrok, W., Davidson, C. I., & Nicholson, K. W. (1996). Dry deposition of particles: Implications and recommendations for mapping of deposition over Europe. *Tellus B: Chemical and Physical Meteorology*, *48*(5), 710-710.

Santoso, M., & Lestiani, D. D. (2014). Application of ED XRF in supporting national program of air quality improvement in Indonesia. XRF Newsletter, 26, 8-13.

Santoso, M., Sutisna, A. T., Darsono, R. M., Lestiani, D. D., Dam astuti, E., Kurniawati, S., & Nasional, B. T. N. (2010). Peran teknik analisis nuklir dalam kesehatan dan lingkungan. In Seminar Nasional Keselamatan dan Lingkungan VI (pp. 31-59).

Sahoo, K., Alanya-Rosenbaum, S., Bergman, R., Abbas, D., & Bilek, E. M. (2021). Environmental and economic assessment of portable systems: Production of wood-briquettes and torrefied-briquettes to generate heat and electricity. Fuels, 2(3), 345-366.

SCB, Population in the country, counties and municipalities on 31 December 2021 and Population Change in 2021 available at https://www.scb.se/en/finding-statistics/statistics-by-subject-area/population/population-composition/population-statistics/pong/tables-and-graphs/population-statistics---year/population-in-the-country-counties-and-municipalities-on-31-december-2021-and-population-change-in-2021/ (accessed on 7 October 2022).

Segersson, D., Johansson, C., & Forsberg, B. (2021). Near-Source Risk Functions for Particulate Matter Are Critical When Assessing the Health Benefits of Local Abatement Strategies. International journal of environmental research and public health, 18(13), 6847.

Seinfeld, J. H. & Pandis, S. N. (2016), Atmospheric chemistry and physics: from air pollution to climate change, John Wiley & Sons, Inc.

Shao, Y., Ishizuka, M., Mikami, M., & Leys, J. F. (2011). Parameterization of size-resolved dust emission and validation with measurements. Journal of Geophysical Research: Atmospheres, 116(D8).

Sofer, T., Baccarelli, A., Cantone, L., Coull, B., Maity, A., Lin, X., & Schwartz, J. (2013). Exposure to airborne particulate matter is associated with methylation pattern in the asthma pathway. Epigenomics, 5(2), 147-154.

Spanne and Gustafsson, 2020 available at
https://malmo.miljobarometern.se/content/docs/Luften_i_Malm%C3%B6_2019.pdf

Squizzato, S., Masiol, M., Rich, D. Q., & Hopke, P. K. (2018). PM2. 5 and gaseous pollutants in New York
State during 2005–2016: Spatial variability, temporal trends, and economic influences. Atmospheric Environment, 183, 209-224.

Su, H., Cheng, Y., & Pöschl, U. (2020). New multiphase chemical processes influencing atmospheric aerosols, air quality, and climate in the anthropocene. Accounts of chemical research, 53(10), 2034-2043.

Swietlicki, E., med flera, 2008. Metaller i svävande stoft i Landskrona – koncentrationer och källor. Rapport LUTFD2/(TFKF-3101)/1-28/(2009), Lunds universitet, Lund, Sverige, Maj 2009.

Tecer, L. H., Alagha, O., Karaca, F., Tuncel, G., & Eldes, N. (2008). Particulate matter (PM2. 5, PM10-2.5, and PM10) and children's hospital admissions for asthma and respiratory diseases: a bidirectional case-crossover study. Journal of Toxicology and Environmental Health, Part A, 71(8), 512-520.

Tegen, I., & Schepanski, K. (2018). Climate feedback on aerosol emission and atmospheric concentrations. Current Climate Change Reports, 4(1), 1-10.

Tremper, A. H., Font, A., Priestman, M., Hamad, S. H., Chung, T. C., Pribadi, A., ... & Green, D. C. (2018). Field and laboratory evaluation of a high time resolution x-ray fluorescence instrument for determining the elemental composition of ambient aerosols. Atmospheric Measurement Techniques, 11(6), 3541-3557.

Trojanowski, R., & Fthenakis, V. (2019). Nanoparticle emissions from residential wood combustion: A critical literature review, characterization, and recommendations. Renewable and Sustainable Energy Reviews, 103, 515-528.

Truncale, T., Harbison, R. D., Bourgeois, M. M., & Johnson, G. T. (2015). Metal fume fever and metal-related lung disease. Hamilton & Hardy's Industrial Toxicology. Sixth. Hoboken, New Jersey: John Wiley & Sons, Inc, 289-300.

Twigg, B. M. V., & Phillips, P. R. (2009). Cleaning the air we breathe-controlling diesel particulate emissions from passenger cars. Platinum Metals Review, 53(1), 27-34.

US-EPA: Environmental Technology Verification Report. Cooper

Environmental Services LLC Xact 625 Particulate Metals Monitor, Report no. EPA/600/R-12/680, by Thomas Kelly and Amy Dindal, Battelle John McKernan, 2012. available at https://archive.epa.gov/nrmrl/archive-etv/web/pdf/p100fk6b.pdf

Van Lith, S. C., Alonso-Ramírez, V., Jensen, P. A., Frandsen, F. J., & Glarborg, P. (2006). Release to the gas phase of inorganic elements during wood combustion. Part 1: development and evaluation of quantification methods. Energy & Fuels, 20(3), 964-978.

Veres, P. R., Neuman, J. A., Bertram, T. H., Assaf, E., Wolfe, G. M., Williamson, C. J., ... & Ryerson, T.
B. (2020). Global airborne sampling reveals a previously unobserved dimethyl sulfide oxidation mechanism in the marine atmosphere. Proceedings of the National Academy of Sciences, 117(9), 4505-4510.

Von der Weiden, S. L., Drewnick, F., & Borrmann, S. J. A. M. T. (2009). Particle Loss Calculator–a new software tool for the assessment of the performance of aerosol inlet systems. Atmospheric Measurement Techniques, 2(2), 479-494.

Wang, F., Yu, H., Wang, Z., Liang, W., Shi, G., Gao, J., ... & Feng, Y. (2021). Review of online source apportionment research based on observation for ambient particulate matter. Science of The Total Environment, 762, 144095.

Watts, P., & Howe, P. (2010). Strontium and strontium compounds (No. 77). World Health Organization.

Wei, B., & Yang, L. (2010). A review of heavy metal contaminations in urban soils, urban road dusts and agricultural soils from China. Microchemical journal, 94(2), 99-107.).

Weinzierl, B., Ansmann, A., Prospero, J. M., Althausen, D., Benker, N., Chouza, F., ... & Walser, A. (2017). The Saharan aerosol long-range transport and aerosol–cloud-interaction experiment: overview and selected highlights. Bulletin of the American Meteorological Society, 98(7), 1427-1451.

WHO (2021) – Fact sheet: Ambient (Outdoor) Air pollution
Available at: https://www.who.int/news-room/fact-sheets/detail/ambient-(outdoor)-air-quality-and-health (Accessed on 2 October 2022).

WHO (2021) – Fact sheet: Household air pollution and health
Available at: https://www.who.int/news-room/factsheets/detail/household-air-pollution-and-health (Accessed on 2 October 2022).

WHO global air quality guidelines. Particulate matter (PM2.5 and PM10), ozone, nitrogen dioxide, sulfur dioxide and carbon monoxide. Geneva: World Health Organization; 2021 (https://apps.who.int/iris/handle/10665/345329).

WHO. Ambient (Outdoor) Air Quality and Health. Key Facts. 2 May 2018. Available online: https://www.who.int/news-room/fact-sheets/detail/ambient-(outdoor)-air-quality-and-health (accessed on 20 September 2022).

Yam, K. M. (2019). Influence from long-distance transport, local sources, and precipitation on black carbon concentrations at a rural background field station in southern Sweden.

Yu, J., Yan, C., Liu, Y., Li, X., Zhou, T., & Zheng, M. (2018). Potassium: a tracer for biomass burning in Beijing? Aerosol and Air Quality Research, 18(9), 2447-2459.

Yu, G., Zhang, Y., Yang, F., He, B., Zhang, C., Zou, Z., ... & Chen, J. (2021). Dynamic Ni/V Ratio in the Ship-Emitted Particles Driven by Multiphase Fuel Oil Regulations in Coastal China. Environmental Science & Technology, 55(22), 15031-15039.

Zhang, J., & Shao, Y. (2014). A new parameterization of dust dry deposition over rough surfaces. Atmos. Chem. Phys. Discuss, 14(6), 8063-8094.

Zhang, R. (2010). Getting to the critical nucleus of aerosol formation. *Science*, *328*(5984), 1366-1367.